

AD-A049 626

AIR FORCE WEAPONS LAB KIRTLAND AFB N MEX  
THERMAL NEUTRON DAMAGE IN BIPOLAR TRANSISTORS.(U)  
DEC 77 T D STANLEY

F/G 9/1

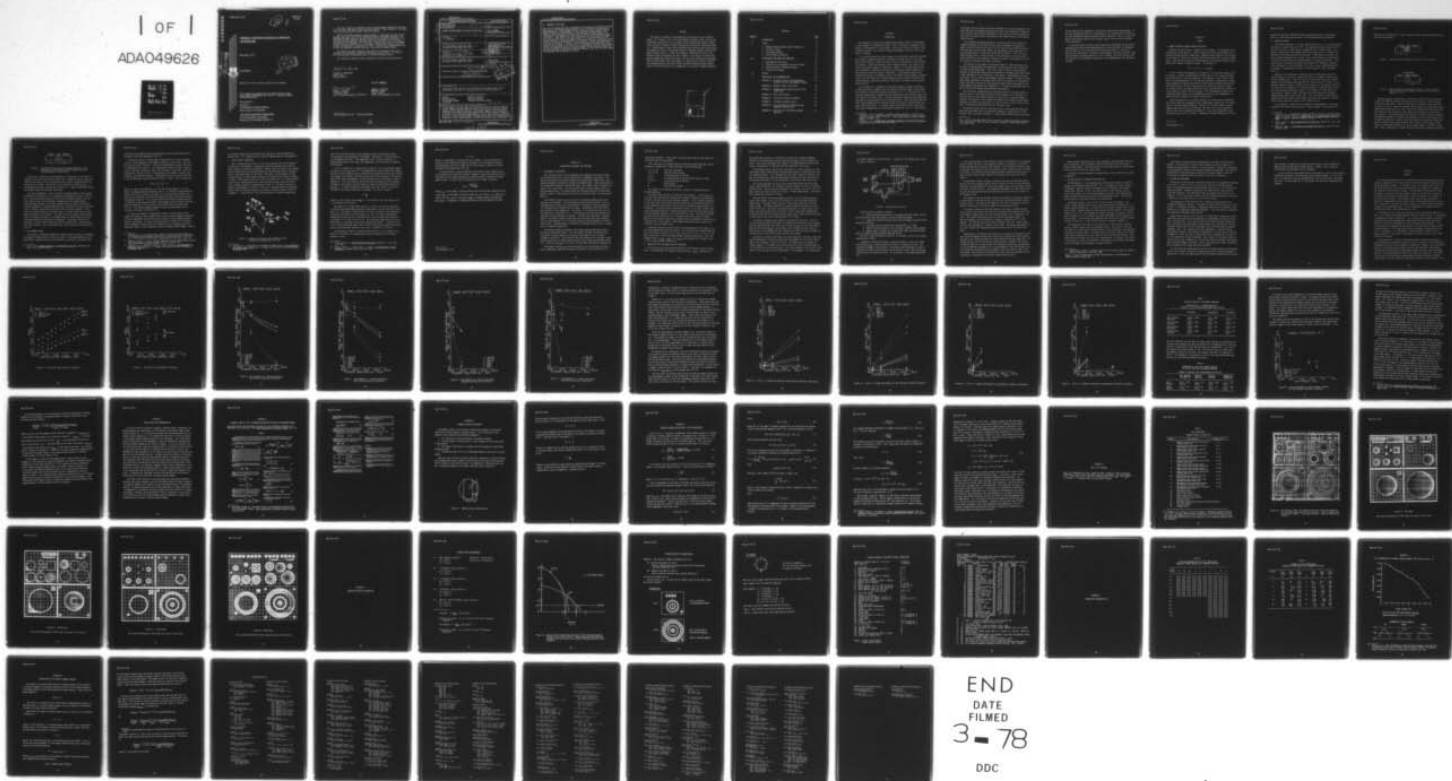
UNCLASSIFIED

AFWL-TR-77-168

NL

| OF |

ADAO49626



AD A 049626

AFWL-TR-77-168

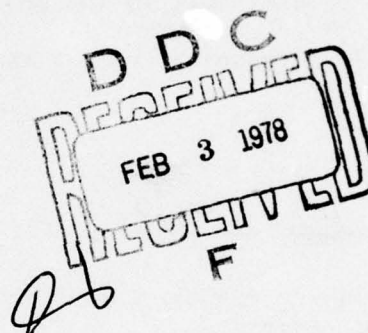
AFWL-TR-  
77-168

12 2

## THERMAL NEUTRON DAMAGE IN BIPOLAR TRANSISTORS

December 1977

Final Report



Approved for public release; distribution unlimited.

This research was sponsored by the Defense Nuclear Agency  
under Subtask Z99QAXTB037, Work Unit 01, "Radiation Effects  
on Microelectronics."

Prepared for  
Director  
DEFENSE NUCLEAR AGENCY  
Washington, DC 20305

AIR FORCE WEAPONS LABORATORY  
Air Force Systems Command  
Kirtland Air Force Base, NM 87117



AD NO. 100 FILE COPY

This final report was prepared by the Air Force Weapons Laboratory, Kirtland Air Force Base, New Mexico, under Job Order 88091132. Major Richard D. Chronister (ELP) was the Laboratory Project Officer-in-Charge.

When US Government drawings, specifications, or other data are used for any purpose other than a definitely related Government procurement operation, the Government thereby incurs no responsibility nor any obligation whatsoever, and the fact that the Government may have formulated, furnished, or in any way supplied the said drawings, specifications, or other data is not to be regarded by implication or otherwise as in any manner licensing the holder or any other person or corporation or conveying any rights or permission to manufacture, use, or sell any patented invention that may in any way be related thereto.

This report has been reviewed by the Office of Information (SUI) and is releasable to the National Technical Information Service (NTIS). At NTIS, it will be available to the general public, including foreign nations.

This technical report has been reviewed and is approved for publication.

*Richard D. Chronister*

RICHARD D. CHRONISTER  
Major, USAF  
Project Officer

FOR THE COMMANDER

*Aaron B. Loggins*

AARON B. LOGGINS  
Lt Colonel, USAF  
Chief, Transient Radiation Effects Br

*Donald A. Dowler*

DONALD A. DOWLER  
Colonel, USAF  
Chief, Electromagnetics Division

DO NOT RETURN THIS COPY. RETAIN OR DESTROY.





SECURITY CLASSIFICATION OF THIS PAGE (When Data Entered)

DDC  
RECEIVED  
FEB 3 1978  
F

LB



UNCLASSIFIED

SECURITY CLASSIFICATION OF THIS PAGE(When Data Entered)

20. ABSTRACT (continued)

each case the damage observed corresponded to the fraction of Boron-10 to total boron used as the emitter dopant material, thus confirming the hypothesized damage mechanism. The dependence of the collector current, thermal neutron fluence, and emitter-base geometry on the observed gain degradation also indicated that bulk damage is responsible for thermal neutron damage in PNP transistors. Some devices were also irradiated in a fast-neutron environment. Fast neutrons were found to be approximately 100 times more effective than thermal neutrons in producing damage in the devices that use a naturally occurring ratio of Boron-10 to Boron-11 in the emitter. Formulas were developed to calculate the fraction of lithium atoms and alpha particles generated in the emitter that do damage in the base, and to calculate the relative effectiveness of fast and thermal neutrons in producing damage in PNP transistors where the combined thickness of the emitter and base regions is less than the path length of a 0.88 MeV lithium nucleus in silicon.

UNCLASSIFIED

SECURITY CLASSIFICATION OF THIS PAGE(When Data Entered)



## CONTENTS

<u>Section</u>		<u>Page</u>
I	INTRODUCTION	5
II	THEORY	8
	1. Damage Producing Thermal Neutron Reactions	8
	2. Transistor Theory	9
	3. Bulk Damage Effects	11
	4. Lattice Defect Production	13
III	EXPERIMENTAL EQUIPMENT AND PROCEDURE	16
	1. Experimental Transistors	16
	2. Transistor Test Equipment and Test Procedure	17
	3. National Bureau of Standards Reactor	21
	4. Irradiation Procedure	22
IV	RESULTS	24
V	CONCLUSIONS AND RECOMMENDATIONS	40
	APPENDIX A: A General Proof of the Degradation Equation for Bulk Displacement Damage	41
	APPENDIX B: Geometry Factor Calculation	43
	APPENDIX C: Thermal Neutron Reaction Rate in PNP Transistors	45
	APPENDIX D: NBS-2 Test Pattern	49
	APPENDIX E: Transistor Process Information	56
	APPENDIX F: Transistor Characteristics	63
	APPENDIX G: Flux Information on Thermal Column Pneumatic Tube Facility	66
	APPENDIX H: Derivation of the Relative Damage Equation	67



## SECTION I

### INTRODUCTION

The detonation of nuclear and thermonuclear weapons results in the release of large numbers of high-energy neutrons. When a transistor is exposed to fast neutrons, displacement of silicon atoms in the crystal lattice structure of the transistor results. As a result of these displacements, the gain of the transistor is reduced.

If in traveling from the nuclear weapon to an electronic system the neutrons pass through a moderating material like water or carbon, they will be slowed until their velocity is about the same as that of the molecules of the surrounding material. These slow neutrons, called thermal neutrons, are unable to do direct displacement damage in transistors. However, it has been observed that some transistors irradiated with thermal neutrons suffer damage comparable to that resulting from fast neutron irradiations. Since thermal neutrons have insufficient energy to do damage directly, the thermal neutron damage is hypothesized to be the result of an energy producing nuclear reaction induced by the thermal neutrons, specifically the  $(n,\alpha)$  reaction in the boron used as emitter dopant material.

Itsu Arimura and C. Rosenberg of the Boeing Aerospace Company indicated in a paper published in December 1973 that they had observed damage in PNP transistors resulting from thermal neutron irradiation (ref. 1). They found that the relative effectiveness of thermal neutrons compared to fast neutrons varied from less than  $10^{-3}$  to nearly unity. They discovered that thermal neutron damage was much less in NPN transistors than in PNP transistors. They also found that thin-base, high-frequency devices are more sensitive to thermal neutrons than wide-base, power transistors. In contrast, power transistors are more sensitive to fast neutron damage than are high-frequency transistors (ref. 2). Additionally,

1. Arimura, I. and C. Rosenberg, "Anomalous Damage Mechanism in PNP Silicon Transistors Due to Thermal Neutrons," IEEE Transactions on Nuclear Science, NS-20 6, December 1973.
2. Ricketts, L. W., Fundamentals of Nuclear Hardening of Electronic Equipment, Wiley-Interscience, Inc., New York, 1972.

the thermal neutron fluence and current dependence of the gain degradation indicated that bulk displacement damage was the most likely degradation mechanism. These findings led Arimura and Rosenberg to the conclusion that the damage was the result of thermal neutron absorption by the Boron-10 atoms in the emitter dopant material.

This hypothesized damage mechanism is consistent with what Arimura and Rosenberg observed and has been seen by several subsequent investigators. Namely, since PNP transistors have  $10^2$  to  $10^4$  more boron than NPN transistors, PNP transistors should suffer greater gain degradation when subjected to a given thermal neutron fluence than should NPN transistors. Also, since the doping concentration is usually higher in high-frequency transistors than in power transistors, high-frequency transistors should be more sensitive to thermal neutron irradiation than power transistors.

The fraction of the atoms in the emitter region of a PNP transistor that are boron is approximately one-thousandth, and the fraction that are Boron-10 is about two ten-thousandths. Also, only a small fraction of the particles produced in the emitter region would be expected to do damage which would result in gain degradation in the transistor's base region. Some tentative calculations by Dr. Vail of the Air Force Weapons Laboratory (AFWL), Kirtland Air Force Base (KAFB), New Mexico, indicated that as few as 20 reactions in the emitter region could have occurred for some reported fluence levels using typical transistor geometry and doping level (appendix C). It seems inconceivable that so few particles could produce observable gain degradation.\*

The Electronics Phenomenology and Technology Branch of the AFWL needed to know the source of the observed thermal neutron damage in PNP transistors to develop a means of performing theoretical calculations of expected damage in radiation environments. They proposed the study of the thermal neutron damage mechanism in bipolar PNP transistors as a thesis topic at the Air Force Institute of Technology, Wright-Patterson Air Force Base, Ohio.

The approach chosen for the investigation was to have some PNP transistors made that were electrically and physically identical, differing only in the isotopic ratio of Boron-10 to Boron-11. These devices would then be irradiated

---

\*Dr. P. Vail of the AFWL, KAFB, NM, has written an unpublished paper concerning the calculation of reaction rate of neutrons absorbed in boron doped transistors, April 1976.

and the observed gain degradation correlated to the Boron-10 concentration. If the gain degradation observed is proportional to the concentration of Boron-10, then the hypothesized damage mechanism would be supported. Also, by having the devices specifically made for this purpose, control over the device geometry would be possible.

In the next section the basic theory required to understand and analyze the hypothesized thermal neutron damage mechanism in PNP transistors is presented. Also included is a short description of transistor operation. Section III describes the transistors, transistor test equipment, and nuclear reactors used; the experimental procedure employed is also included. The final sections give the results of the experiment, conclusions, and recommendations for additional research.

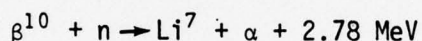


## SECTION II

## THEORY

## 1. DAMAGE PRODUCING THERMAL NEUTRON REACTIONS

Naturally occurring boron is composed of two isotopes: 19.78 percent Boron-10 and 80.22 percent Boron-11. Boron-10 atoms have a very high probability of capturing thermal neutrons (3840 barns) compared to most materials and in particular to Boron-11, which has a thermal neutron activation cross section of 0.005 barns. When a Boron-10 absorbs a thermal neutron, an exothermic reaction takes place which releases 2.78 MeV of energy. The reaction is



In this reaction the probability of forming  $\text{Li}^7$  in the ground state is only 6.4 percent. Usually an intermediate excited state of  $\text{Li}^7$  is formed followed by the emission of a 0.48 MeV gamma ray. The remainder of the 2.78 MeV (2.30 MeV) is divided between the  $\text{Li}^7$  and the alpha particle. Conservation of momentum considerations leads to the division of the remaining energy such that the alpha particle has 1.47 MeV of energy and the lithium ion receives 0.88 MeV. The lithium nucleus and alpha particle fly apart, dissipating their energies in a few microns of crystal lattice structure. The displacements caused by the lithium and alpha recoils are the hypothesized source of gain degradation in thermal neutron irradiation of bipolar transistors.\*

Since the absorption of a thermal neutron by a silicon atom can transmute the silicon atom into a phosphorus atom, transmutation doping has to be considered as a possible damage mechanism. However, silicon has a thermal neutron capture cross section of only 0.09 barns; and out of 100 neutron captures in silicon, only 4 are transmuted to phosphorus. Also, the transmutation takes place with a half life of 2.6 hours. Absorption of thermal neutrons by silicon

---

\* See footnote, p. 6.

produces an average of 780 MeV of kinetic energy applied to a silicon atom (ref. 3). Thus, while not promising, silicon capture must be considered.

## 2. TRANSISTOR THEORY

The bipolar transistor is a current amplifying device. It is a three-region device and is usually made of silicon. The regions are made by doping the silicon with boron for a p-type region or phosphorus for an n-type region. In p regions the majority of the charge carriers are holes, while in n regions the majority of the charge carriers are electrons. A PNP transistor consists of two p regions separated by an n region. One p region doped to a concentration of about  $10^{16}$  boron atoms per cubic centimeter is called the collector. The n region, which is doped to a concentration of about  $10^{18}$  phosphorus atoms per cubic centimeter, is called the base. The final p region, called the emitter, is doped to a concentration of about  $10^{20}$  boron atoms per cubic centimeter (ref. 4).

Because of the difference in majority carrier concentration across the region boundaries, diffusion currents will flow in an attempt to balance the carrier concentrations. These currents will continue to flow until internal potentials are developed that cause the net flow of carriers to cease. If an external potential source is supplied to the junction of two regions with polarity such that the formation of an internal potential is opposed, then current will flow through the potential source. This condition is referred to as a forward bias. Figure 1 shows a PNP transistor with forward bias potential applied between the emitter and the base. Since the emitter is more heavily doped than the base, most of the current flow across the junction is from the flow of holes from the p region to the n region (ref. 5).

If a potential is applied so as to enhance the development of an internal potential, the flow of charge carriers is almost stopped. This situation is

3. Cleland, J. W., "Transmutation Doping and Recoil Effects in Semiconductors Exposed to Thermal Neutrons," Proceedings of the International Enrico Fermi School of Physics, Radiation Damage in Solids, Academic Press, New York, 1962.
4. Brophy, James J., Basic Electronics for Scientists, McGraw Hill, Inc., New York, 1969.
5. McKelvey, John P., Solid State and Semiconductor Physics, Harper and Row, New York, 1966.

referred to as reverse bias. Figure 2 shows a reverse bias applied between the base and the collector.

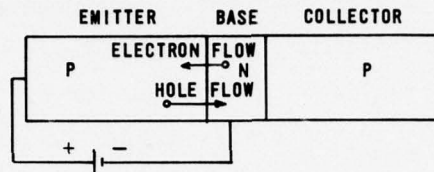


Figure 1. Forward Biased Emitter-Base Junction in PNP Transistor

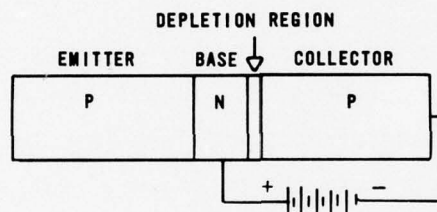


Figure 2. Reverse Biased Collector-Base Junction in PNP Transistor: Only the Few Carriers Thermally Generated in the Depletion Region Will Flow.

The base region in transistors is very thin (on the order of 0.5 microns), so that the diffusion length of minority carriers, holes, is longer than the width of the base region. When the transistor is biased for normal operation as shown in figure 3, holes are injected into the base region across the forward biased emitter base junction. Most of the holes diffuse right through the thin base region and are collected in the reverse bias potential of the collector-base junction. Since the collector-base junction is reverse biased, increasing the potential between the collector and the base will have little effect on the collector current flow. However, since the forward bias potential between the emitter and base controls the diffusion flow of holes into the base, a small change in emitter-base potential can cause a large change in collector current flow. Thus, a power gain in signals can be achieved using transistor amplifiers.



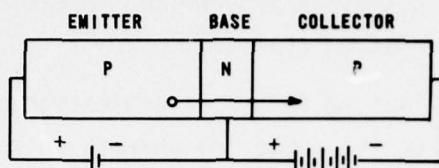


Figure 3. The PNP Transistor Biased for Normal Operation: Holes Generated in the Emitter Diffuse Through the Base and Are Accumulated in the Collector.

The DC gain, a measure of relative merit of a transistor, is the ratio of collector current flow to the base current flow. Ideally the base current flow should be very small, giving a large gain, but in actual practice the DC gain ranges from 20 to 1000. The DC gain is also referred to as Beta and  $H_{FE}$ . To be completely specified, the gain must be given for a specific collector current and voltage between the collector and emitter.

Since gain degradation is one of the most important effects of the neutron irradiation of transistors, it is important to understand the origin of the DC gain. There are several sources of base current including injection of electrons from the base into the emitter, leakage across the reverse biased collector-based junction, and surface currents from the emitter to the base. The main component is usually recombination of a portion of the holes with electrons in the base region before they can diffuse into the collector. Since holes are minority carriers in the base region, it seems likely that the holes would all combine with electrons. This does not occur, however, since recombination of electrons and holes is forbidden except at lattice defect sites due to quantum mechanical conservation requirements. These defect sites may be impurities or energy level changes resulting from vacancies or interstitials in the crystal lattice. Many such defects exist in even the best silicon crystals (ref. 6).

### 3. BULK DAMAGE EFFECTS

Fast-neutron irradiation degrades the transistor gain directly by increasing the number of lattice defects in the base region. Even though defects are produced evenly throughout the transistor material, only those in the base region

6. Larin, Frank, Radiation Effects in Semiconductor Devices, John Wiley and Sons, Inc., New York, 1968.

(and the two thin-depletion regions separating the base from the emitter and collector) cause gain degradation (ref. 7).

The minority carrier lifetime before recombination of a hole in N-doped silicon is thus dependent on the number of defects in the silicon. One over the minority carrier lifetime is called the recombination rate per carrier and is symbolized by the letter R. The recombination rate per carrier is proportional to the base current and, hence, the reciprocal of the gain. Also, the recombination rate per carrier is proportional to the number of defects and, therefore, the radiation exposure. Recombination rate per carrier is the sum of the recombination rates of different origins. Hence, it can be shown that

$$\Delta(1/\beta) = \frac{1}{\beta_f} - \frac{1}{\beta_i} = C\phi$$

where  $\beta_f$  is gain after exposure,  $\beta_i$  is the gain before exposure,  $\phi$  is the fluence of damage producing radiations, and C is a constant of proportionality. Another form of this equation, referred to as the bulk damage equation, has been used for many years to predict the expected change in gain resulting from fast-neutrons exposure. The C, usually called the radiation damage constant, is dependent on the energy and type of displacement causing radiation, and the physical properties of the transistor, most notably the base transit time (ref. 8). The radiation damage constant (C) has also been shown to be a function of collector current (ref. 9).

As long as the number of recombination centers is proportional to the fluence of radiation, and no other effect (such as surface leakage or mechanical failure) predominates and significant gain remains, the bulk damage equation should be applicable. As long as the concentration of Boron-10 is not appreciably decreased by thermal neutron irradiation, the bulk damage equation is expected to apply to the hypothesized source of thermal neutron damage. However,

7. Donovan, R. P., J. R. Hauser and M. Simon, "A Survey of the Vulnerability of Contemporary Semiconductor Components to Nuclear Radiation," AFWL-TR-74-61, Air Force Avionics Laboratory, Wright-Patterson AFB, Ohio, June 1974.
8. Ramsey, C. and Dr. P. Vail, "Current Dependence of the Neutron Damage Factor," IEEE Transactions on Nuclear Science, NS-17 6, December 1970.
9. Crawford, J. H., "Radiation Effects in Ionic Crystals," The Interaction of Radiation with Solids, ed., R. Stumae, North Holland Publishing Company, Amsterdam, 1964.

the radiation damage constant would be very sensitive to device geometry and doping levels. For a general proof of the bulk damage equation, see appendix A.

#### 4. LATTICE DEFECT PRODUCTION

When a charged particle moves in a lattice structure, most of the energy of the particle is dissipated in interactions with the electrons of the lattice atoms, causing no lattice displacements. However, when the energy of the charged particle falls below the threshold energy for the particular lattice structure, atomic interactions begin to take place. The result is displacement of atoms leaving vacancies in some lattice positions and interstitials (excess of atoms) in others. The threshold energy in silicon is 145 keV (ref. 9). Atoms displaced by the initial charged particle may have sufficient energy to displace other atoms, thereby producing a cascade effect (figure 4). The energy required to produce a displacement in silicon is 12.9 eV, so a charged particle with energy greater than the threshold energy could produce a maximum of about 11,000 displacements. A large portion of the atoms displaced in radiation damage moves

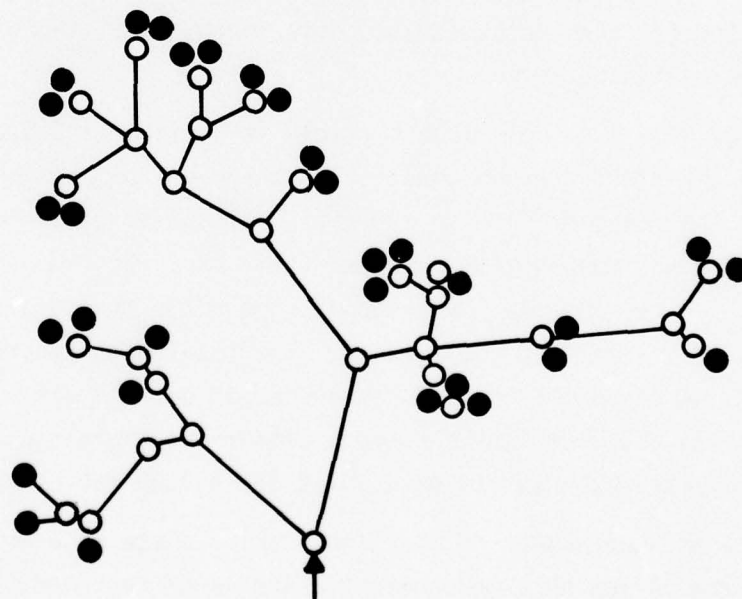


Figure 4. Example of a Crystal Lattice Damage Cascade:  
○ Vacancy, ● Interstitials (ref. 10)

10. Leibfried, G., "Introduction into Radiation Damage Theory," The Interaction of Radiation with Solids, ed., R. Stumae, North Holland Publishing Company, Amsterdam, 1964.



back into lattice positions or form complexes (such as divacancies) within milliseconds of the occurrence of the damage. The result is a partial healing of the damaged transistor. This phenomenon, which is called annealing, is temperature sensitive; the higher the temperature, the more rapid and complete the annealing.

If it is assumed that a charged particle does all of its displacement damage at the end of its path, and if it is assumed that the path length of the charged particle is small compared to the surface area of the device so that semi-infinite slab geometry can be used, then the portion of particles produced in the emitter region that cause displacements in the base region can be calculated as shown in appendix B. Also, the range of the particle must be greater than the combined thickness of the emitter and base regions to apply the relationship derived in appendix B. If these assumptions can be made, then the fraction of particles produced in the emitter region that do damage in the base is given by

$$G = \frac{h}{2R}$$

where  $G$  is the fraction doing damage,  $h$  is the width of the base region, and  $R$  is the range of the particle.

The range of a 1.47 MeV alpha particle in silicon is 5.5  $\mu\text{m}$  as determined by applying the Bragg-Kleeman equation to the range of an alpha particle in air (ref. 11). The range of lithium nuclei in silicon is given in ion implantation literature for various initial energies (ref. 12). By linear interpolation between the 300 keV and the 1 MeV ranges, one finds the total path length for a 0.88 MeV Li in silicon to be 3.12  $\mu\text{m}$ . The total path length should, for this application, be corrected to give the projected path length. A correction factor of 0.96 was obtained, again using a linear interpolation between data points, giving a projected path length of 3.00  $\mu\text{m}$  for a 0.88 MeV Li in silicon.

To calculate the number of reactions taking place in a unit volume as the result of irradiation by a monoenergetic source of neutrons, the following equation is used

11. Price, William J., Nuclear Radiation Detection, McGraw-Hill, Inc., New York, 1964.
12. Davies, John A., L. Erikson and J. W. Mayer, Ion Implantation in Semiconductors, Academic Press, New York, 1970.

$$R = \sigma N \phi$$

where  $R$  is the number of reactions per unit volume,  $\sigma$  is the reaction cross section for the reaction and energy of interest,  $N$  is the number of atoms of reacting material per unit volume, and  $\phi$  is the fluence of neutrons to which the material was exposed per unit area.

For distributions of neutron energies, the problem is more complex since cross sections are functions of energy. Appendix C shows the derivation of the reactions per unit volume resulting from thermal neutron irradiation of boron doped silicon. For this case the reaction per unit volume is given by

$$R_{\alpha, \text{Li}} = \frac{N_{\text{B10}} \sigma_0 \phi}{1.128}$$

where  $R_{\alpha, \text{Li}}$  is the number of alpha particles and lithium atoms produced per unit volume,  $N_{\text{B10}}$  is the number of Boron-10 atoms per unit volume,  $\sigma_0$  is 3840 barns =  $3.84 \times 10^{-21} \text{ cm}^2$ , and  $\phi$  is the total number of thermal neutrons incident per unit area.\* In appendix C a sample calculation using this equation is given.

---

\* See footnote, p. 6.

### SECTION III

#### EXPERIMENTAL EQUIPMENT AND PROCEDURE

##### 1. EXPERIMENTAL TRANSISTORS

The transistors used in this experiment were produced at the Device Design and Processing Division of Sandia Laboratories, Albuquerque, New Mexico. The devices were made in an Extrion Automated Ion-implantation Chamber using a test pattern produced by the National Bureau of Standards (NBS). Since the process of ion-implantation separates isotopes by weight, the isotopic ratio of Boron-10 to Boron-11 was controllable. The devices were made in three isotopic ratios of emitter-dopant atoms: 100 percent Boron-10, 20 percent Boron-10 and 80 percent Boron-11 (which is approximately the naturally occurring ratio), and 100 percent Boron-11.

Two different times were used to drive in the emitter dopant atoms after they were ion implanted. Since the base had previously been driven in for an extended period of time, only the thickness of the emitter region was appreciably affected by the different drive-in times. Consequently, the transistors were available in two geometries: (a) emitter  $1.1\text{ }\mu\text{m}$  and the base  $0.5\text{ }\mu\text{m}$ , and (b) emitter  $0.9\text{ }\mu\text{m}$  and base  $0.7\text{ }\mu\text{m}$ . The narrow-base devices are referred to as high-gain and the wide-base as low-gain. For both cases the number of dopant atoms in the emitter region was the same since the boron atoms were implanted with a surface density of  $5 \times 10^{15}$  boron atoms per square centimeter of emitter surface area. Complete process information with doping profiles and pin arrangement is included in appendix D.

The National Bureau of Standards test pattern used was NBS-2 described in NBS Special Publication 400-6. This test pattern includes 20 different test structures including capacitors, resistors, and diodes as well as several different transistors. The structures that were bonded out for use were a small emitter transistor, an emitter sheet resistor, and a large area tetrode transistor. These are structures 7, 15, and 19 on the NBS-2 test pattern (appendix E).

The tetrode transistor has two base contacts, one at the center and one at the circumference, enabling the device to be used as a base resistor or as a



large area transistor. Since there is no passivation mask with the NBS-2 set, the devices were not passivated.

Thus, there were 12 different types of transistors made which were distinguished by a number and a letter according to the following code:

2, 6, or 10	Low Gain (wide base)
4, 8, or 12	High Gain (narrow base)
2 or 4	100 percent Boron-11 emitter
6 or 8	20 percent Boron-10 and 80 percent Boron-11 emitter
10 or 12	100 percent Boron-10 emitter
A	Small emitter
B	Large emitter tetrode

For example, a 2B transistor would be a low-gain, 100 percent Boron-11 tetrode transistor.

The devices were supplied in eight-lead T0-5 packages. A field plate contact over the collector-base junction was included in addition to the emitter, collector, and base (two for the tetrode) contacts. Since a changing potential on the field plate could affect the device operation and radiation sensitivity, it was soldered to the collector lead so that a consistent potential would be maintained. The leads going to the emitter resistor in the small emitter transistor package were bent 90° forward and spaced so that they could make contact with four adjacent contacts in an eight-lead T0-5 socket. The transistor leads were bent so that they would fit in a standard four-lead transistor socket. Devices of each specific type were assigned consecutive numbers to enable unique identification of each device. These numbers were painted on the top of the transistor case with enamel paint.

The three transistors of each variety were characterized on the AFWL's Fairchild 600 Computerized Transistor Testor. The characteristics measured were the gain at collector currents of 0.01, 0.02, 0.05, 0.1, 0.2, 0.5, 1, 2, 5, 10, and 20 milliamps with 5 volts maintained between collector and emitter. Also, the leakage currents  $I_{(CBO)}$ ,  $I_{(EBO)}$ , and  $I_{(CEO)}$  were measured with voltages of 10, 3, and 10 volts applied, respectively.

## 2. TRANSISTOR TEST EQUIPMENT AND TEST PROCEDURE

The 72 devices were characterized before and after thermal neutron irradiations. The characteristics measured included DC gain,  $I_{(EBO)}$ , capacitance of

the emitter-base junction as a function of reverse bias voltage, breakdown voltage of the emitter-base junction, emitter resistance, and base sheet resistance. Also, scope photographs were taken of the common emitter characteristic curves as displayed on a Tektronik Type 575 Transistor Curve Tracer.

The equipment used to measure gain consisted of a current regulator, a regulated power supply, three digital voltage-current meters, a transistor test box, and connecting cables. This equipment was also used to measure saturation voltage, the voltage drop across the emitter-base junction, the base resistance for the tetrode transistors, and the resistance of the emitter sheet resistances.

The current regulator was built using a Kepco Operational Amplifier power supply, model OPS100-2TA. It supplied a constant current for use as a collector current source. The current was selectable in two ranges, from 0.25 to 10 milliamps, and was set with a precision, 10-turn, 1-kilohm potentiometer. The compliance voltage was limited to 15 volts.

The base current source was formed by placing a high resistance (approximately 100 kilohms) in series with the output of a well-regulated laboratory power supply. The power supply used was a Trygon Electronics Dual Lab Power Supply, DL40-1. The power supply had an output voltage continuously variable from 0 to 40 volts. The series resistance consisted of a fixed, 2-watt, wire-wound, 10-kilohm resistor and a precision, 10-turn, 500-kilohm potentiometer. By adjusting the series resistance and the power supply output voltage, the base current could be set from a few microamps to 4 milliamps.

The series resistances were housed in the transistor test box. This box also contained switches which enable the voltage being monitored to be switched from the voltage between the emitter and collector ( $V_{CE}$ ) to the voltage between the base and emitter ( $V_{BE}$ ) or the voltage across the emitter sheet resistor. The test box also contained the jacks necessary to attach the other equipment to the transistor or the emitter sheet resistor being tested.

The digital voltage-current meters used were Honeywell's Digitest, Model 333, Digital Multimeters. These are three-digit instruments with full-scale ranges down to 99.9 microamps or 99.9 millivolts. The maximum error of reading on current ranges is 1.5 percent plus or minus one digit, and on voltage ranges it is 0.5 percent plus or minus one digit. The input impedance on the 10-volt scale (which is the one used for gain measurements) is 100 megohms. The voltage drop

for current readings is 100 millivolts. A diagram of the complete test circuit is given in figure 5.

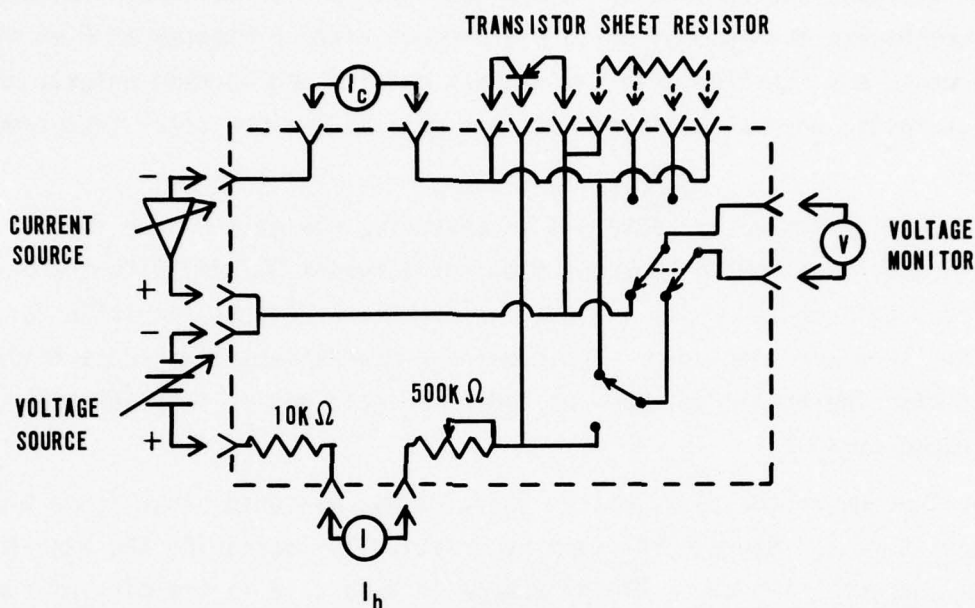


Figure 5. Transistor Test Circuit

Transistor gain is tested as follows:

- a. After placing the transistor in the transistor test socket, turn up the base current until the reading is several hundred microamps.
- b. Adjust the collector current source for the highest current at which the gain is desired.
- c. Turn down the base current until the desired  $V_{CE}$  is read.
- d. Record the base current for the collector, current, and  $V_{CE}$  chosen.
- e. Repeat steps b through d for successively lower collector currents until all desired operating points have been tested.

The gain is then calculated by dividing the collector current by the corresponding base current.

To measure a saturation voltage, a similar procedure is used; only rather than setting a  $V_{CE}$ , a base current which results in saturation is set. The saturation voltage is read directly. The emitter sheet resistance is read by setting the collector current source for the desired current, then reading the voltage across the emitter resistor. The resistance is calculated using Ohm's law.



It was observed that if the collector current is maintained over an extended period of time, the gain of the transistor appears to increase as a result of thermal drifting due to internal ohmic heating. The drifting was found to cause an apparent gain increase of up to 8.5 percent after 5 minutes at 6 mA of collector current. By starting with the highest current and working quickly down to lower currents, thermal drift effects are minimized since total test time is reduced.

An additional problem, observed in measuring the gain of the large emitter devices, was large leakage current flow (as large as 0.7 mA) with the base open. Therefore, gain measurements for the large emitter devices for collector currents less than 1 mA were not used. The remaining measurements for these devices must be used with the knowledge that the indicated gain may be high as a result of the leakage current.

The leakage of the base emitter junction was measured since gamma irradiation of transistors can degrade the gain by drastically increasing the base emitter leakage current. The cause of the damage in this case is trapping of ions produced in the surface of the device above the emitter-base junction.

The method of measuring the base leakage was to apply a constant reverse bias voltage to the emitter-base junction and measure the leakage current flow. The constant voltage source used was a mercury battery with an output of 1.35 volts. The current was measured using a Keithley Instruments, Model 153, Microvolt-ammeter, which was capable of reading currents from  $10^{-1}$  to  $10^{-11}$  amperes. The accuracy was plus or minus 4 percent on the  $10^{-11}$  ampere scale, with an input impedance of 1 megohm on that range. The battery was housed in a box with a switch that removed the battery from the circuit for zeroing the meter.

Capacitance of the emitter-base junction as a function of reverse bias voltage, and the breakdown voltage, and voltage of the emitter-base junction were measured using a Boonton Electronics Direct Capacitance Bridge, Model 750. The voltage applied to the transistor was monitored with a Honeywell three-digit Voltmeter, Model 33, and the current flow through the transistor was monitored with an ME-70A/PSM-6 Standard US Air Force Multimeter on the 100 microamp scale. The information obtained with this equipment, while not directly used in the experiment, helps to verify the similarity of the electrical properties of the transistors, irrespective of the boron isotope used for doping.

Common emitter characteristics of the transistors were recorded before and after irradiation, using a Tektronic Type 575 Transistor Curve Tracer and a Polaroid Scope Camera. These characteristic curves were taken as a backup data source and were not used as a data source.

A summary of the preirradiation characteristics of the transistors is given in appendix F.

### 3. NATIONAL BUREAU OF STANDARDS (NBS) REACTOR

The NBS Reactor is a  $D_2O$  moderated and cooled reactor located in the NBS complex at Gaithersburg, Maryland (ref. 13). It operates at a power output of 10 megawatts (thermal) using 5.4 kilograms of fuel enriched to 93 percent Uranium 235. The fuel is split into two sections so that fissions are not taking place directly in front of experimental facilities, thus reducing the gamma ray and fast neutron exposures in the experimental areas. The facility was designed for high thermal neutron flux experiments.

The thermal column is a 54- by 52- by 37-inch block of graphite. The thermal column pneumatic tube facility was used to expose the transistors to thermal neutron irradiation. In this facility the copper cadmium ratio is 3415, which implies a thermal neutron to fast neutron ratio of 30,000.\* The absolute neutron flux is  $1.6 \times 10^{11}$  neutrons per square centimeter per second, so that total fluences of  $5 \times 10^{15}$  neutrons per square centimeter can be accumulated in about 8 hours. The thermal column pneumatic tube facility was carefully characterized in June 1971. A copy of this finding is included in appendix G.

The transistors were sent into the reactor--in a small plastic container called a rabbit--along a series of pneumatic tubes. The length of time that the rabbit is in the reactor is determined by a timer installed in the pneumatic tube facility control panel. The timer used in the control panel can be chosen from several different full-scale ranges to allow more accurate setting. When setting near full-scale, the accuracy is approximately  $\pm 2$  percent. The rabbits are returned to a lead pig so that their radioactivity can be monitored without excessive exposure of the operator to gamma radiation.

13. "NBS Reactor," Public Information Sheet on the National Bureau of Standards Reactor, Gaithersburg, Maryland, 1969.

\* Raby, T., private communication on the characteristics of the NBS Reactor Thermal Column, 22 June 1976.

Fast-neutron irradiations were accomplished in the SPR-II Sandia Pulsed Reactor. This reactor is a bare critical assembly so that the spectrum of neutron energies produced is nearly a fission spectrum. Using sulfur dosimetry, a 1-MeV-equivalent fluence for the neutron exposure was obtained. The relative effectiveness of fast and thermal neutrons in producing damage in the test transistors was obtained using the results of the fast irradiations.

#### 4. IRRADIATION PROCEDURE

One device of each type was irradiated successively to accumulative fluences of  $5 \times 10^{11}$ ,  $5 \times 10^{12}$ ,  $5 \times 10^{13}$ , and  $2 \times 10^{14}$ , and all but the 100 percent Boron-10 and 20 percent Boron-10 large-emitter devices to  $5 \times 10^{14}$  neutrons per square centimeter. Between irradiations, the common emitter characteristic curves were observed. No significant change was detected for the first two fluences. For the last three fluences, gain and leakage measurements were made in addition to the characteristic curves that were taken.

The temperature of the devices during irradiation was monitored using Tempilable Temperature Monitors. The range covered by these monitors was 130° F to 160° F in 10-degree increments. Temperature monitoring was important, since annealing is a temperature dependent phenomenon. Also, the times of irradiation and subsequent measurement were recorded.

Based on the finding of the first set of irradiations, fluences were calculated that would produce gain degradations of approximately 20 percent, 40 percent, and 60 percent. Two of each of the small-emitter high-gain transistors were irradiated to the calculated fluences except for all the Boron-11 devices. The upper fluence limit for this experiment, set by the NBS Radiation Hazards Committee, was  $5 \times 10^{15}$  neutrons per square centimeter. Since the fluence calculated to produce a 20 percent gain degradation in all the Boron-11 devices exceeded this limit, only two of these devices were irradiated to a fluence of  $5 \times 10^{15}$  neutrons per square centimeter. One of each of the remaining types of transistors was also irradiated to a fluence calculated to produce a gain degradation of approximately 60 percent. Due to time constraints, these irradiations were performed by NBS reactor operations personnel.

To insure that the damage observed was due to thermal neutrons and not gamma rays or fast neutrons, one device of each type was to be irradiated wrapped in cadmium foil. Since the cadmium would block out thermal neutrons while allowing



fast neutrons and gamma rays to penetrate the devices, any gain degradation observed would not be due to thermal neutrons. However, due to technical difficulties this experiment was not performed.

To insure that no stray potentials were developed as a result of the ionizing radiations, the leads of the transistors were shorted together. For the first sets of irradiations, this was accomplished by inserting the leads into conductive foam. For the second set of irradiations, the transistor leads were bent together.

## SECTION IV

## RESULTS

The initial characteristics of the devices confirm that they are electrically similar, regardless of the isotopic ratio of Boron-10 to Boron-11 atoms used as the emitter dopant material. In figures 6 and 7, the average initial gains (of the three transistors of each type characterized) are plotted as a function of the logarithm of the collector current. The deviations (of the gains of three transistors in each set from the average for the set) varied from 4 percent to 12 percent for the small emitter devices, and from 5 percent to 17 percent for the large emitter devices. These graphs, taken from the data presented in appendix F, demonstrate that the initial gains of the transistors, which differ only in the ratio of Boron-10 to Boron-11 used as the emitter dopant, correspond to within one standard deviation. The gain measurements correspond within 1.5 standard deviation to those obtained by Dr. Vail.

The fraction of the initial gain remaining (after each thermal neutron irradiation as a function of thermal neutron fluence for the first set of irradiations) is presented in figures 8 through 11. As is shown on these graphs, the 100 percent Boron-10 devices degraded with roughly one-fifth the fluence required to produce a similar gain degradation in the 20 percent Boron-10 devices. Also, no significant gain degradation was observed in the all-Boron-11 devices at the maximum fluence ( $5 \times 10^{14}$  neutrons per square centimeter) achieved during this set of irradiations. The uncertainty in the measurements of gain, which is about 5 percent, is the source of the apparent increase in gain in some of the all-Boron-11 devices.

The large-emitter, low-gain, 100 percent Boron-11 transistor appeared to have suffered a gain degradation after its first irradiation, with no additional degradation occurring for the remaining irradiations. However, since the characteristic curve photos show no change from the preirradiation to the maximum irradiation, and since the 2-mA measurement showed no change, it was concluded that the initial measurement of the gain for this device was high. The source of the high initial gain reading was probably thermal drift due to a several minute delay in measuring the gain after applying power to the transistor. The

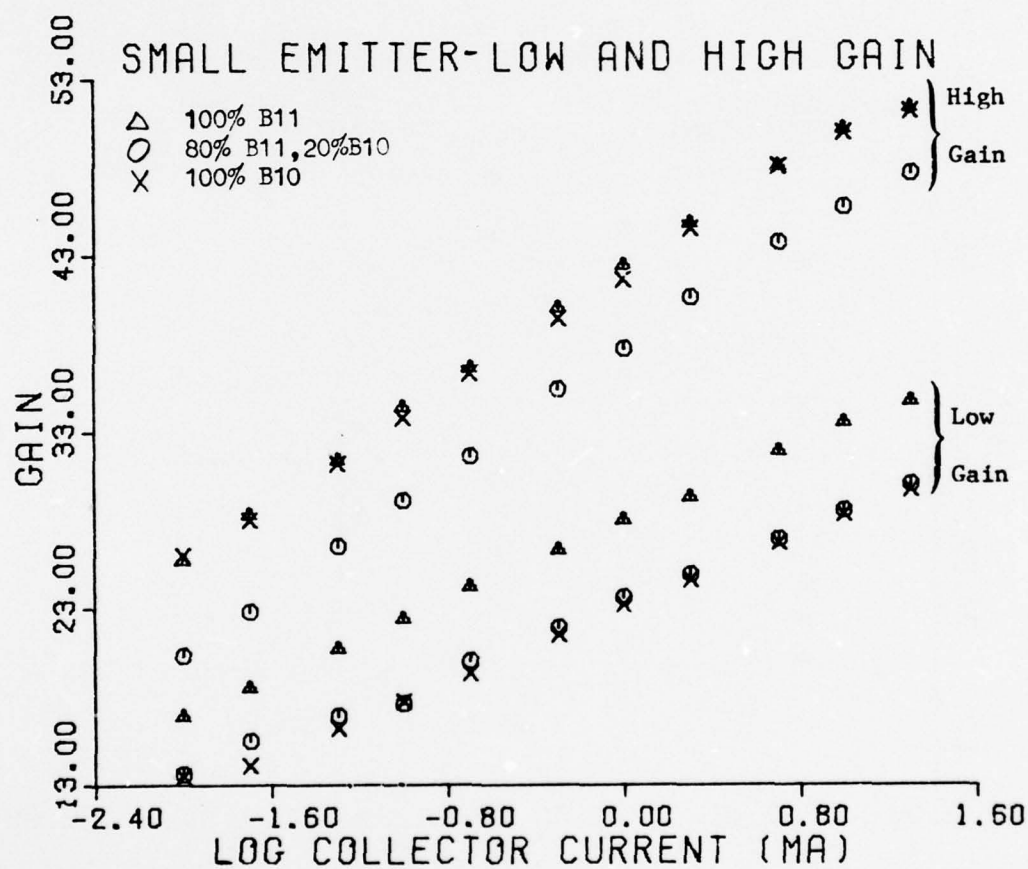


Figure 6. Initial Gain, Small-Emitter Transistors



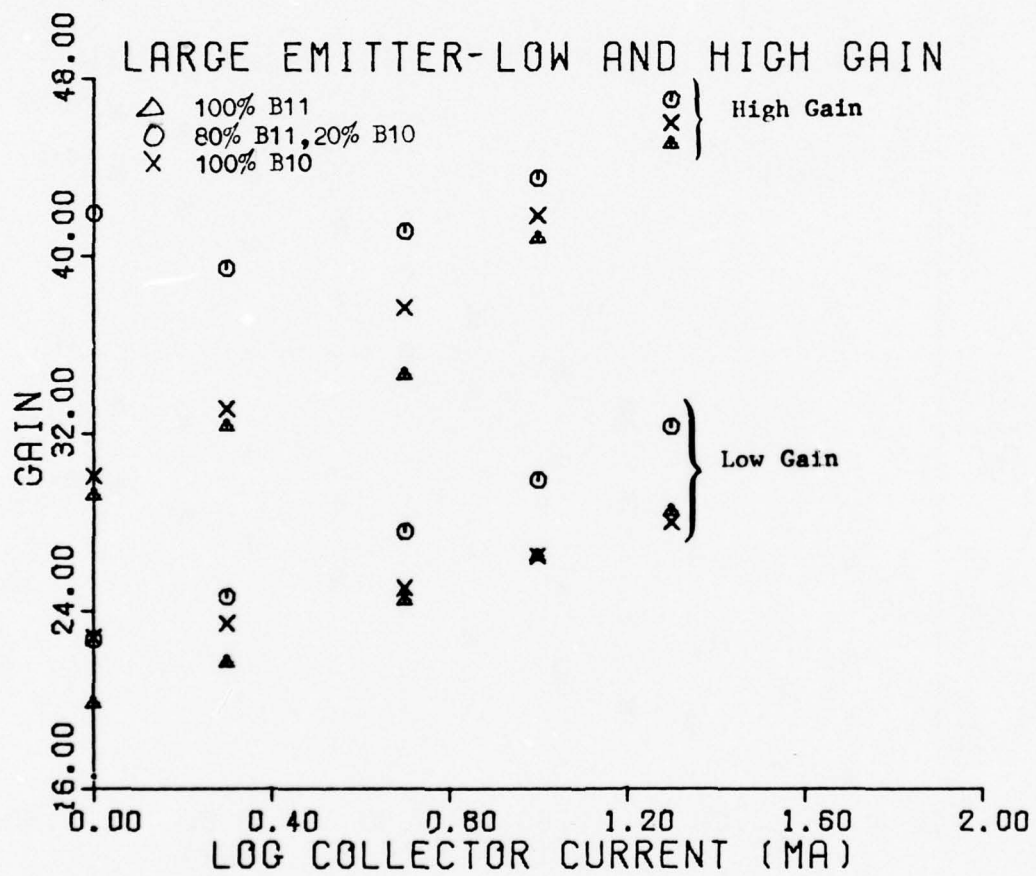


Figure 7. Initial Gain, Large-Emitter Transistors

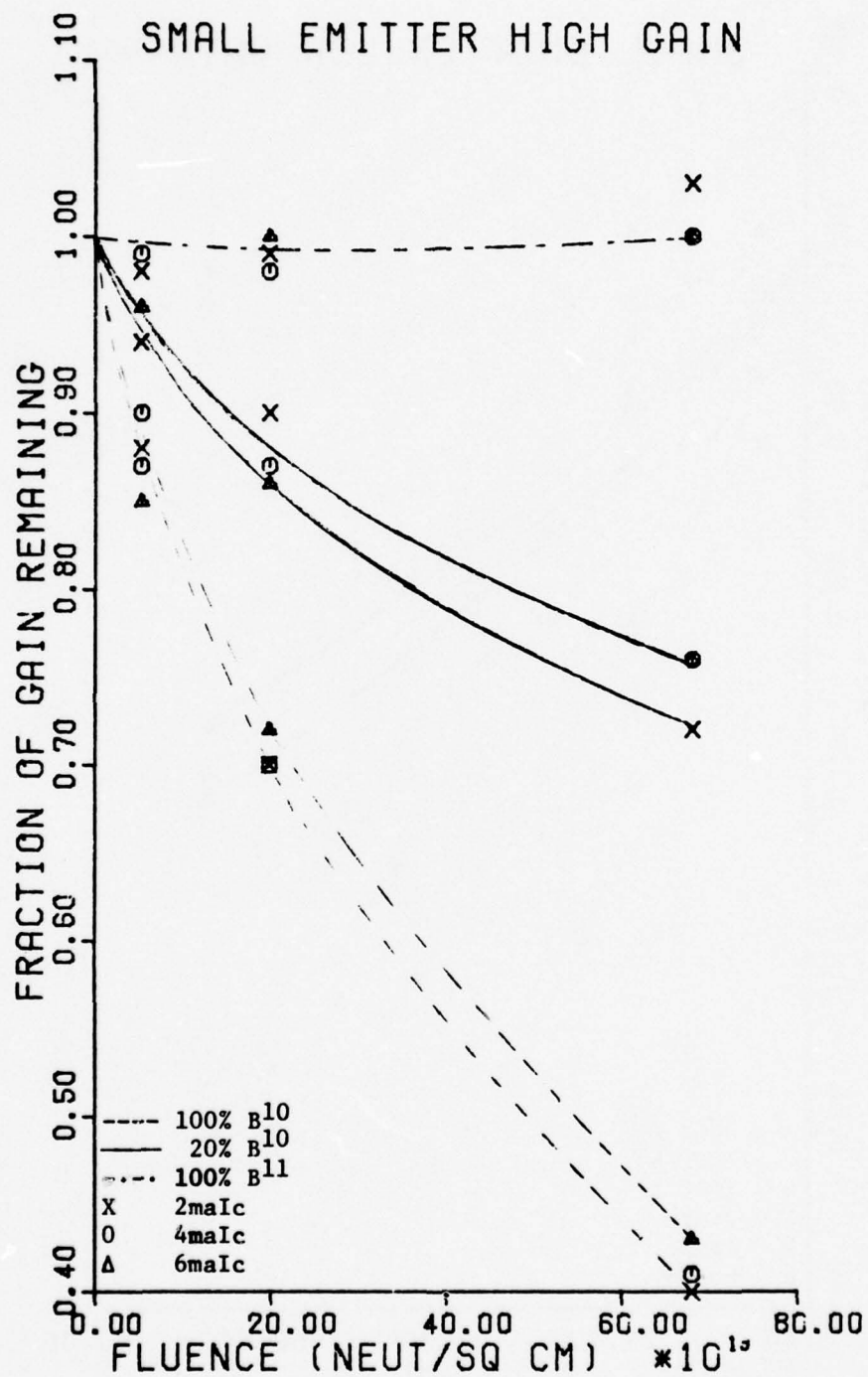


Figure 8. Gain Remaining vs. Fluence and Doping;  
Small-Emitter High-Gain Transistors

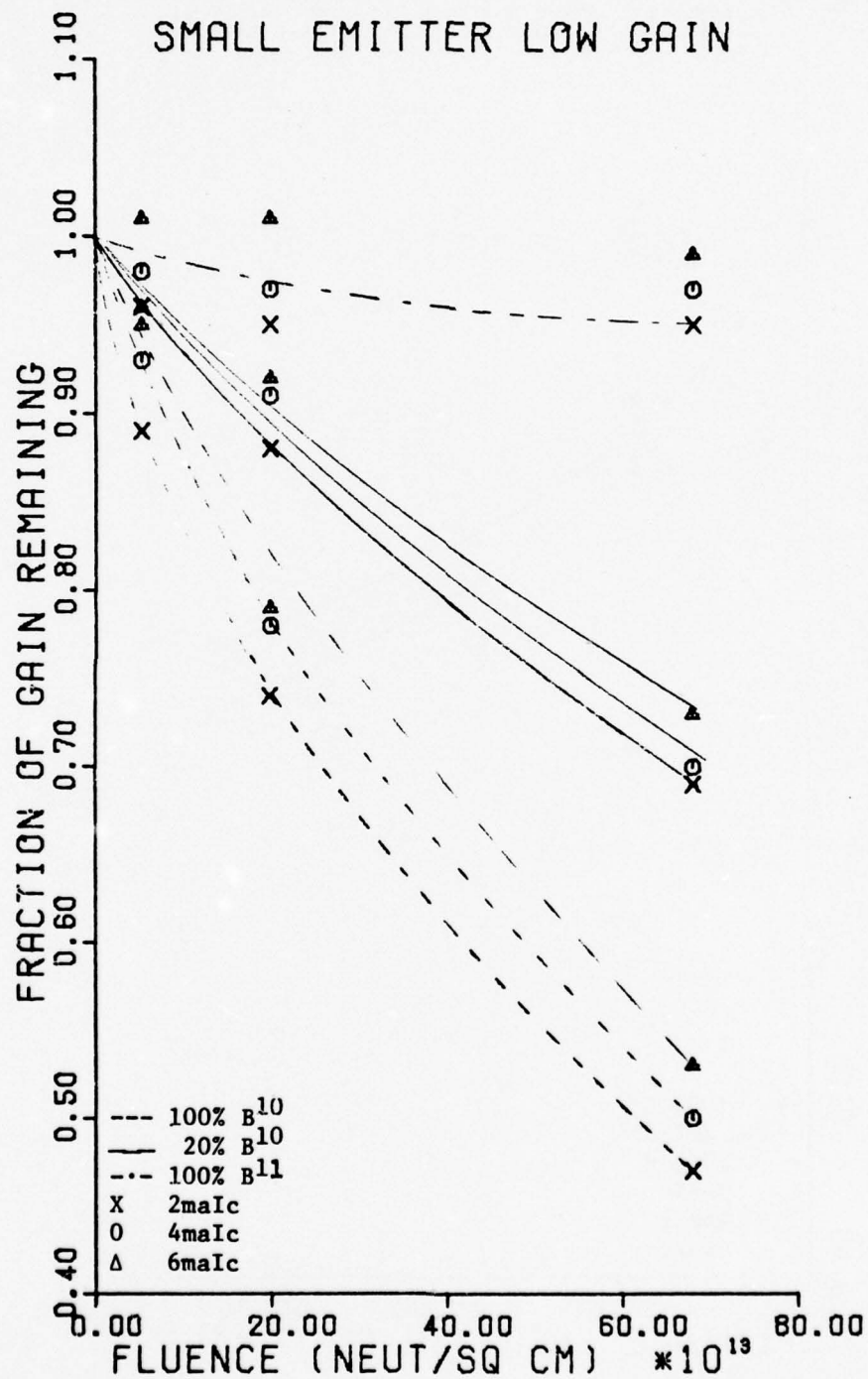


Figure 9. Gain Remaining vs. Fluence and Doping;  
Small-Emitter Low-Gain Transistors



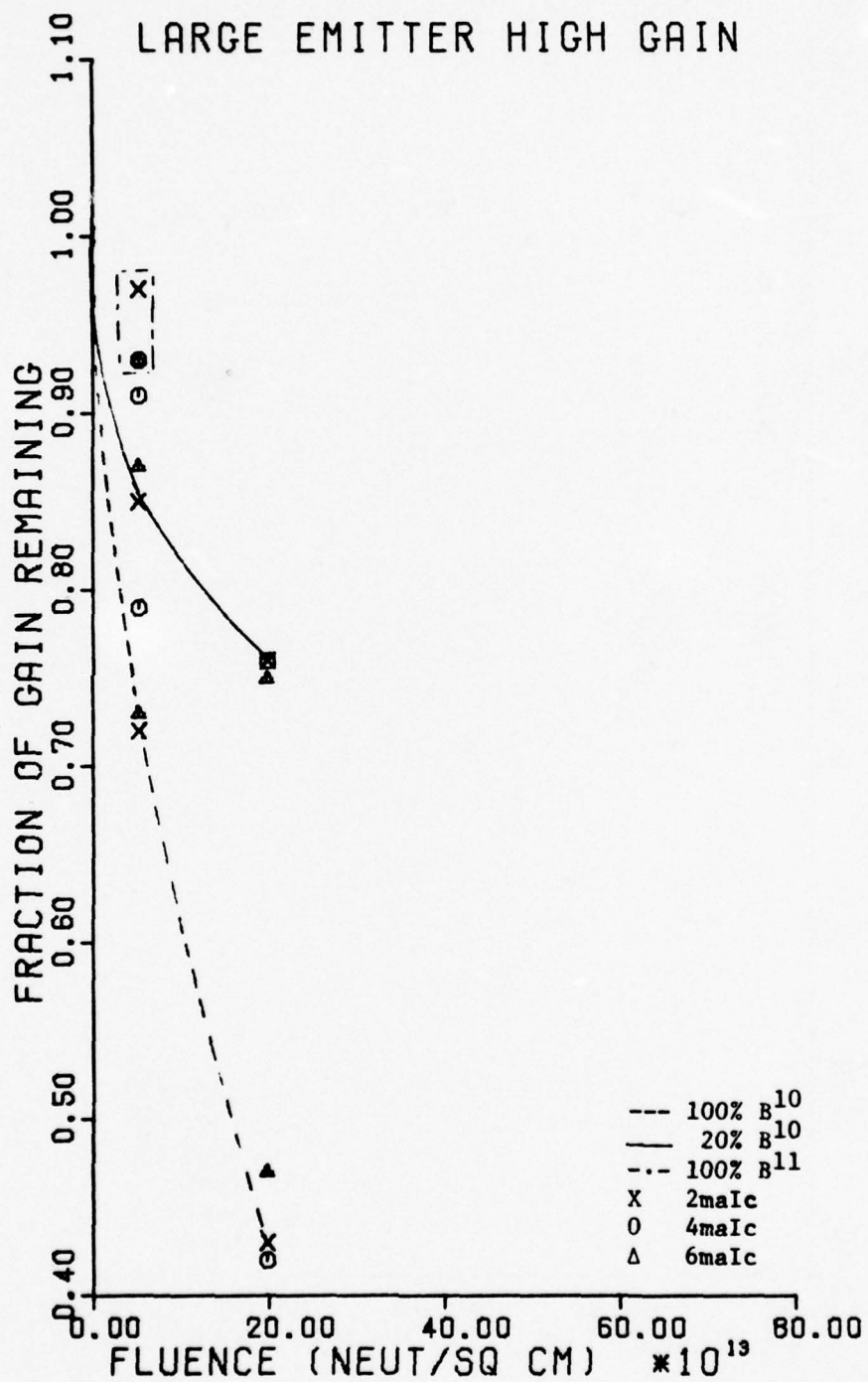


Figure 10. Gain Remaining vs. Fluence and Doping;  
Large-Emitter High-Gain Transistors

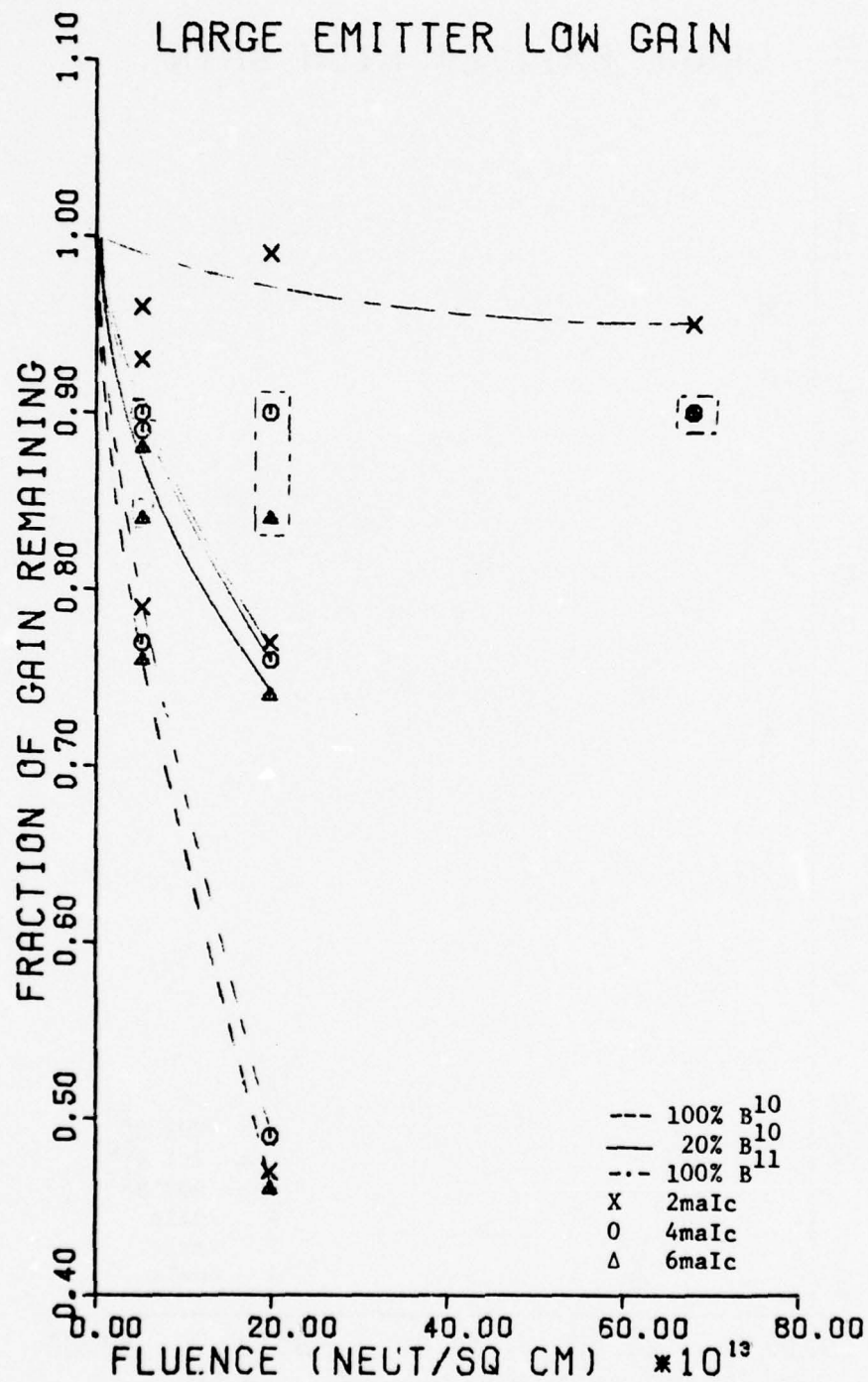


Figure 11. Gain Remaining vs. Fluence and Doping;  
Large-Emitter Low-Gain Transistors

large-emitter, high-gain, 100 percent Boron-11 transistor of this irradiation set failed due to an open circuit in the base (possibly due to mechanical shock in the rabbit tube). For this reason there was only one available data set plotted.

Figures 12, 13, 14, and 15 are graphs of  $\Delta(1/\beta)$  as a function of thermal neutron fluence, also for the first set of irradiations. These graphs show that the damage, as measured by the reciprocal of the gain change  $[\Delta(1/\beta)]$  resulting from a given thermal neutron fluence, follows the bulk damage equation. In other words, the fact that  $\Delta(1/\beta)$  is linearly proportional to the thermal neutron fluence, with the intercept at the origin, indicates that the source of the observed damage is bulk displacement damage. These graphs also show that the wider base transistors (i.e., those with low gain) are more susceptible to thermal neutron damage than the narrow-base (high-gain) transistors, as is expected. For those cases where the gain of the 100 percent Boron-11 transistors appeared to have slightly increased as a result of neutron irradiation, the  $\Delta(1/\beta)$  was set equal to zero.

Since the proportionality constant between  $\Delta(1/\beta)$  and neutron fluence is the radiation damage constant (C), the slopes of the curves are a measurement of C. The greater the damage, the smaller the percent error due to uncertainties in the measurements. Since the uncertainties in the relative values of the flux and in the gain measurements are on the order of 5 percent, those points near the horizontal axis are less reliable than those where the gain degradation is greater than 10 percent.

The second set of irradiations, which were performed by operations personnel of the National Bureau of Standards Reactor, were used to calculate the radiation damage constants for the various combinations of emitter dopant material and device geometry used. They were also compared with bulk damage constants for the fast neutron irradiations performed to obtain the relative effectiveness of fast and thermal neutrons in producing gain degradation in these devices. A summary of these results is given in table 1. Note the close agreement of the values of  $C_{20\%B10}/C_{B10}$  to the expected value of 0.20.

Since the high- and low-gain devices have the same base dopant density and the same geometry, except for the differences in the width of the base regions, their relative values of initial gain and damage constants should be in the same ratio as the square of the base widths. This follows from the fact that



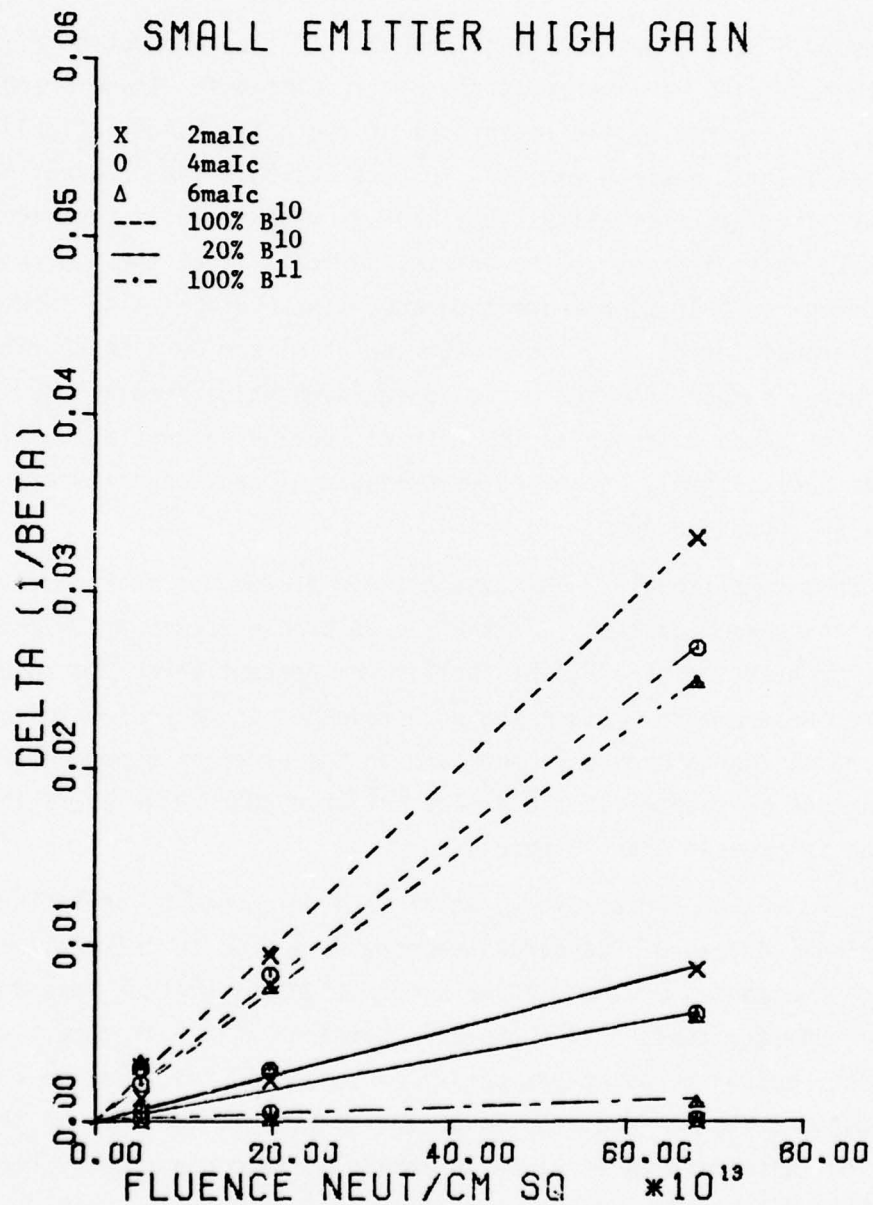


Figure 12.  $\Delta(1/\beta)$  vs. Fluence and Doping for Small-Emitter High-Gain Transistors

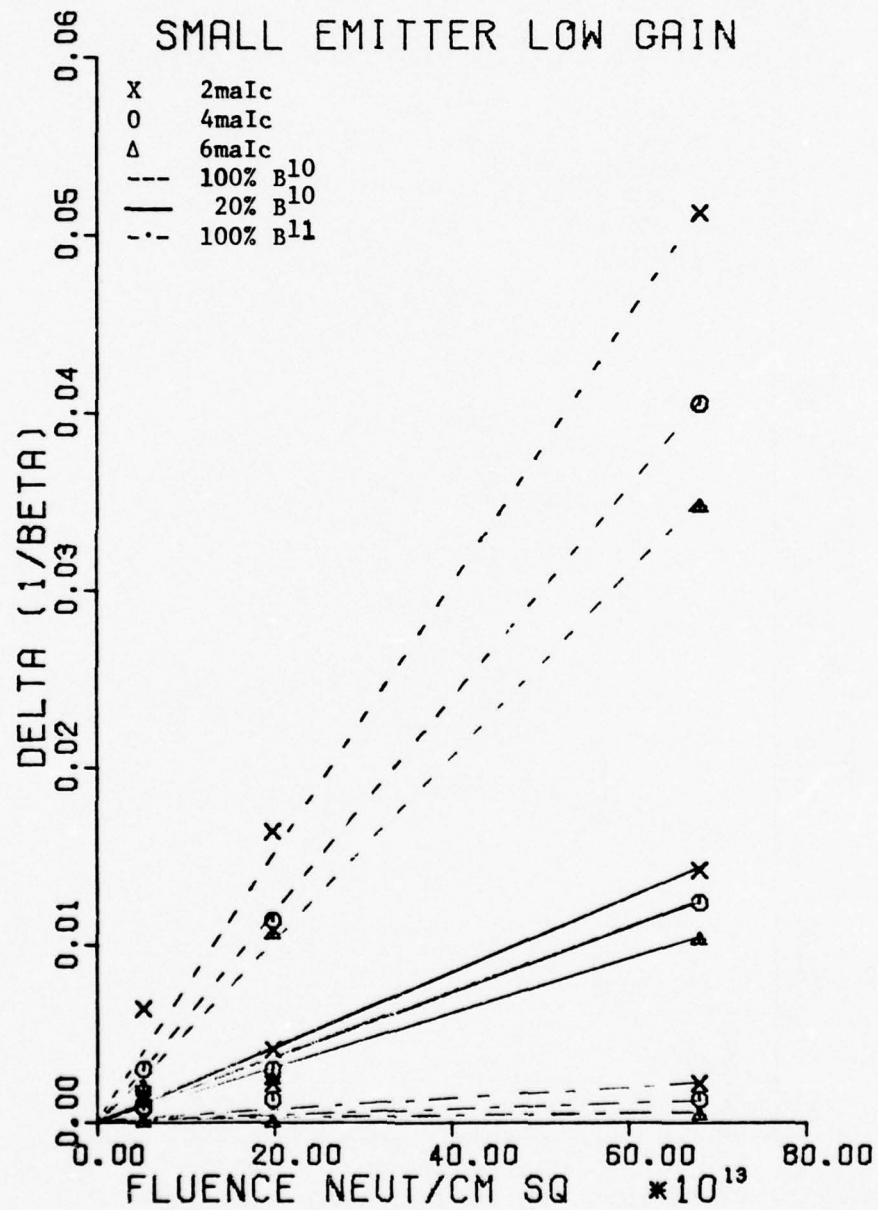


Figure 13.  $\Delta(1/\beta)$  vs. Fluence and Doping for Small-Emitter Low-Gain Transistors

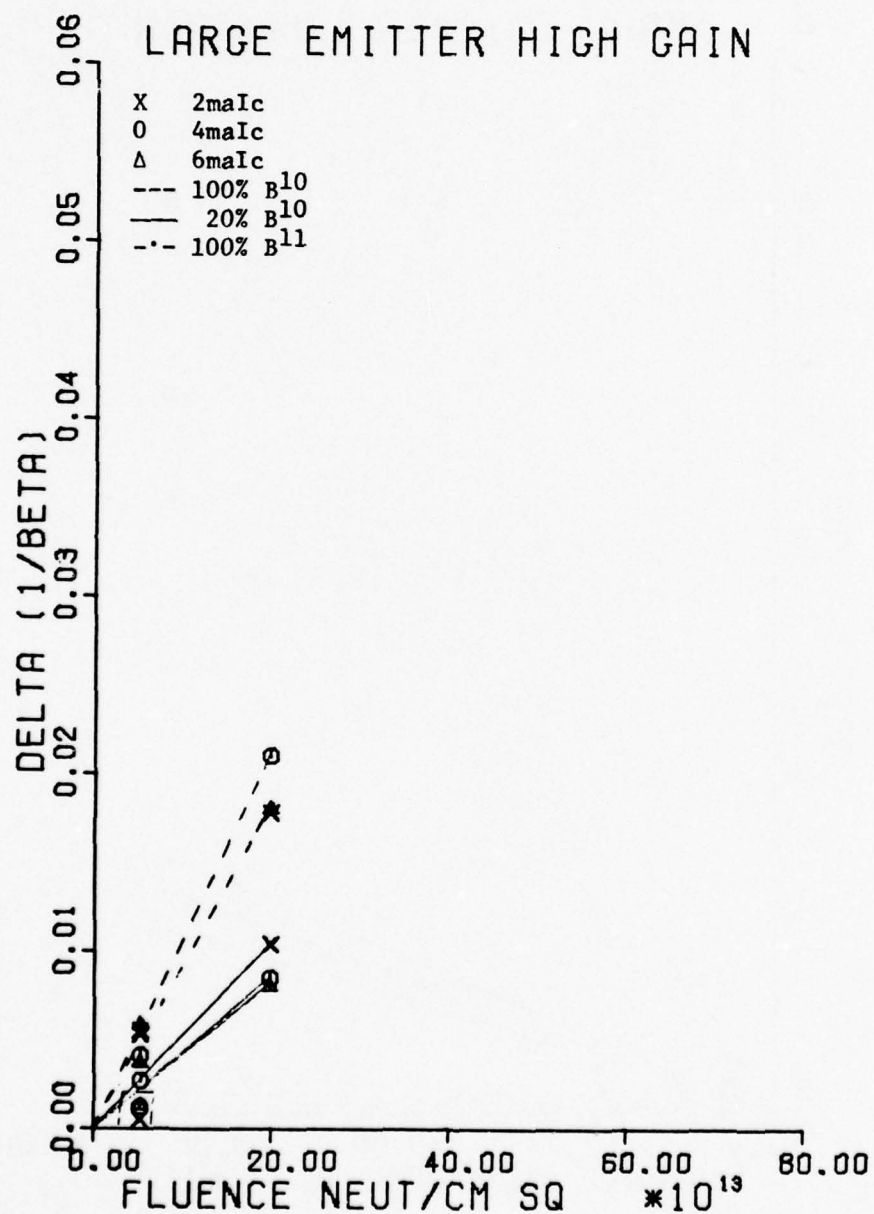


Figure 14.  $\Delta(1/\beta)$  vs. Fluence and Doping for Large-Emitter High-Gain Transistors



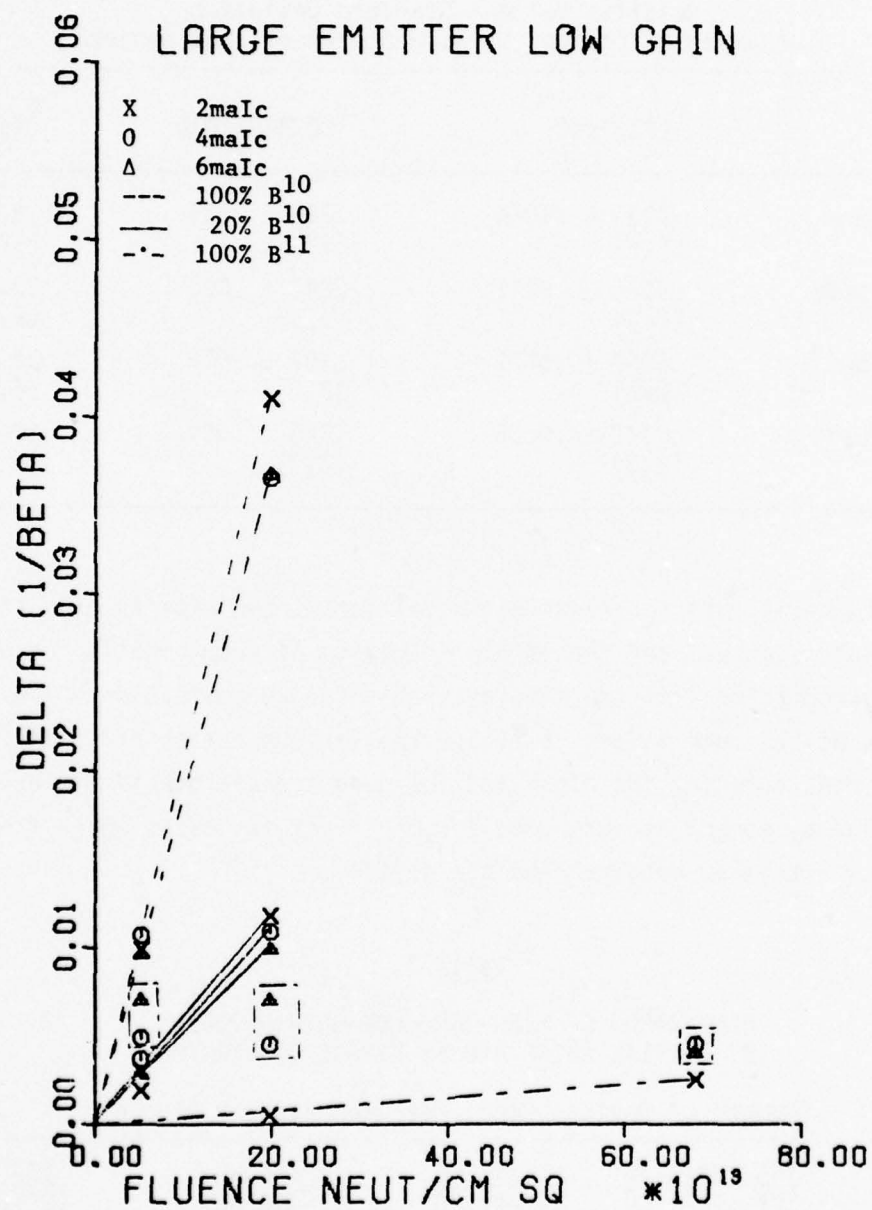


Figure 15.  $\Delta(1/\beta)$  vs. Fluence and Doping for Large-Emitter Low-Gain Transistors

Table 1

## RELATIVE VALUES OF THE DAMAGE CONSTANTS

Relative Value - Standard Deviation  
(Number of Devices Used, Measurements per Device)

	$C_{B11}/C_{B10}$	$C_{20\%B10}/C_{B10}$	$C_{fast}/C_{B10}$
small emitter high gain	$.0233 \pm .0044$ (5,5)	$.190 \pm .035$ (12,4)	$18.2 \pm 1.42$ (12,4)
small emitter low gain	$.0306 \pm .0017$ (2,3)	$.243 \pm .003$ (2,3)	$22.6 \pm 4.07$ (4,1)
large emitter high gain	$.0198 \pm .0007$ (2,3)	$.197 \pm .015$ (2,3)	$22.8 \pm 3.88$ (4,1)
large emitter low gain	$.0142 \pm .0025$ (2,3)	$.143 \pm .004$ (2,3)	$22.9 \pm 4.8$ (4,1)

the time a minority carrier takes to travel across the base is proportional to the base width squared, and that the probability of recombination of a minority carrier is proportional to the time available for recombination. The ratio of the squares of the base widths is 1.65. The various ratios of initial gains and damage constants for the high- and low-gain transistors is summarized in table 2. The agreement is very good for the first two cases where there were many devices with many measurements per device.

Table 2

COMPARISON OF HIGH- AND LOW-GAIN DEVICES  
BY INITIAL GAINS AND BY DAMAGE CONSTANTS

(Number of Devices Used, Measurements per Device)

	$\frac{\text{int. gain HG}}{\text{int. gain LG}}$	$\frac{C_{fast HG}}{C_{fast LG}}$	$\frac{C_{B10 HG}}{C_{B10 LG}}$	$\frac{C_{20\%B10 HG}}{C_{20\%B10 LG}}$
small emitter	$1.65 \pm .153$ (18,11)	$1.43 \pm .26$ (18,4)	$1.80 \pm .025$ (6,3)	$2.10 \pm .011$ (6,3)
large emitter	$1.51 \pm .182$ (17,5)	$1.59 \pm .33$ (17,3)	$1.62 \pm .10$ (6,3)	$2.27 \pm .388$ (6,3)

In figure 16 the current dependence of the various damage constants of the small-emitter high-gain transistor is shown. The damage constants were normalized to those of the 100 percent Boron-10 by multiplying each datum point by the quotient of the average Boron-10 damage constant and the average of the damage constants to be normalized. The normalization factors used are given in the figure. This figure demonstrates that the current dependence of the damage produced by the thermal neutrons is similar to that produced by fast neutrons. Insufficient comparable data points existed to make this comparison for the other transistor geometries.

The emitter and base resistances, as well as the emitter-base junction capacitances as a function of voltage and breakdown voltage of the emitter-base junction, showed no significant change as a result of the irradiations. In all

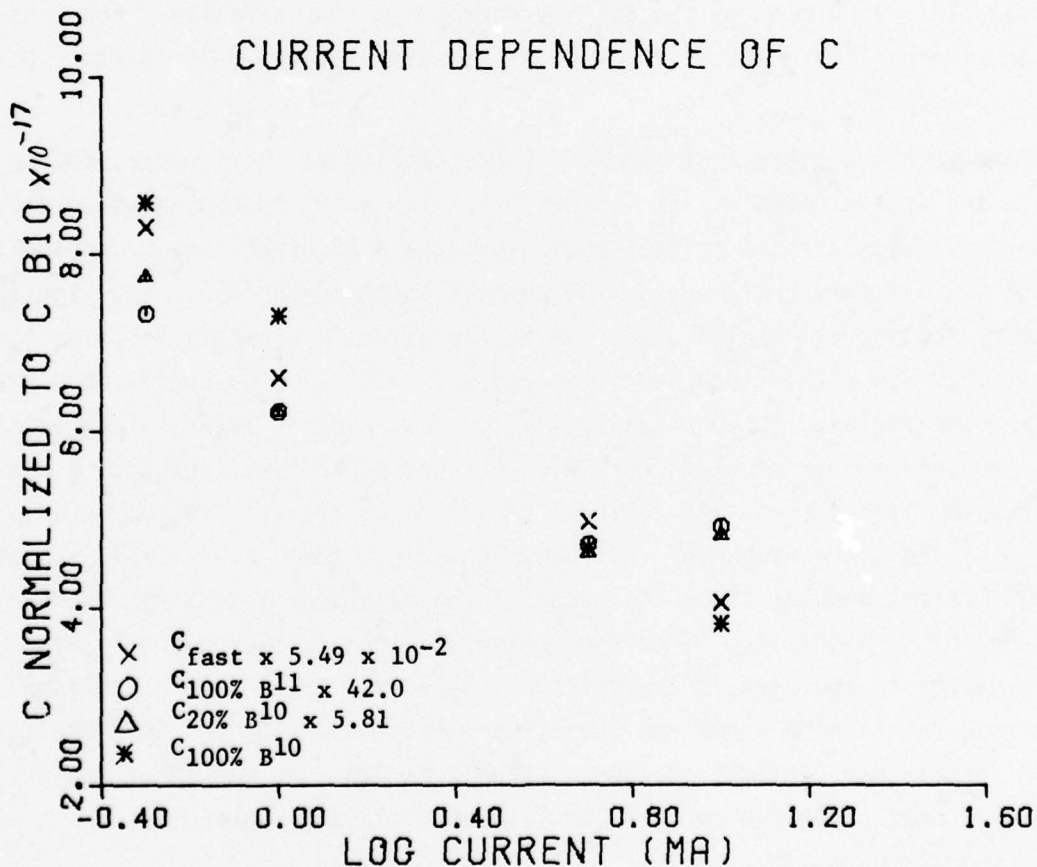


Figure 16. Current Dependence of Various Damage Constants for Small-Emitter High-Gain Transistors



but one of the 100 percent Boron-10, small-emitter, high-gain devices, the emitter-base junction leakage changed less than 50 percent. However, in the devices mentioned, the leakage went from 40 picoamperes to  $4.2 \times 10^6$  picoamperes. As a result of this catastrophic leakage failure, the gain of this device went nearly to zero. In one of the 100 percent Boron-11 large-emitter devices, the collector and emitter contacts appeared to have become shorted together. Two additional devices appeared to have developed open circuits in one or more contacts. The source of these catastrophic failures is unknown.

The temperature monitors in the rabbit tubes indicated that the temperatures of the transistors stayed below 130° F during irradiation so that annealing effects should have been minimized. For the first set of irradiations, the postirradiation gains were measured within 6 hours of the irradiation; and for the second set, 1 week elapsed between the irradiation and the gain measurement. A recheck of one 100 percent Boron-10 device indicated that after 10 days had elapsed,  $12 \pm 3$  percent of the initial damage had been annealed. For this reason, the devices in each irradiation set were compared only to other devices in the same set.

When the calculations of appendix C are applied to the fluence, doping level, and device geometry, it is found that  $1.3 \times 10^6$  thermal neutron captures by Boron-10 atoms in the emitter region produce a 50 percent gain degradation in the small-emitter, high-gain, 100 percent Boron-10 devices. Applying the geometry factors calculated using the method given in appendix B, gives the result that  $5.6 \times 10^4$  alpha particles and  $1.1 \times 10^5$  lithium nuclei do damage in the base region. In contrast,  $5.1 \times 10^4$  fast neutron interactions in the base produce similar results (ref. 9). A 1-MeV neutron will produce  $5.0 \times 10^3$  defects in silicon (ref. 14). Since the volume of the base region is only  $6.4 \times 10^{-9}$  cm<sup>3</sup>, the number of fast-neutron defects would be  $4.0 \times 10^{16}$  cm. As this defect density is on the order of the base dopant density observable degradation is expected. Since the number of alpha particles and lithium atoms doing damage in the base is approximately 3.3 times greater than the fast neutrons, the lithium atoms and the alpha particles would need to produce only 2,000 defects per particle to cause the same damage. As was shown in section II, 11,000 defects per alpha particle or lithium nucleus are possible.

---

14. Buehler, Martin G., Microelectronic Test Patterns: An Overview, NBS Special Publication 400-6, National Bureau of Standards, Washington, DC, August 1974.

The following equation for calculating the relative effectiveness of thermal neutrons to fast neutrons in producing defects in bipolar transistors can be obtained from these results.

$$\frac{C_{\text{thermal}}}{C_{1 \text{ MeV}}} = \frac{0.3 (G_{\alpha} + G_{\text{Li}}) \sigma_{\text{thermal B10}} N_{\text{B10}} W_{\text{Emitter}}}{\sigma_{1 \text{ MeV si}} N_{\text{si}} W_{\text{Base}}}$$

where  $G_{\alpha}$  and  $G_{\text{Li}}$  are the geometry factors derived in appendix B,  $\sigma_{\text{thermal B10}}$  is the Thermal Group capture cross section for Boron-10,  $\sigma_{1 \text{ MeV si}}$  is the one MeV scatter cross section for silicon,  $N_{\text{B10}}$  is the atom density of Boron-10 atoms in the emitter,  $N_{\text{si}}$  is the atom density of silicon in the base,  $W_{\text{Emitter}}$  is the width of the emitter, and  $W_{\text{Base}}$  is the width of the base. This formula, which is derived in appendix H, is good only for devices where the combined width of the emitter and base regions is less than the path length of a 0.88 MeV lithium nucleus in silicon (about 3.0  $\mu\text{m}$ ).

At the fluence at which the 100 percent Boron-11 devices begin to show damage ( $5 \times 10^{15}$  neutrons per square centimeter), the density of thermal neutron captures by silicon atoms would be  $2.3 \times 10^{13}$  captures per square centimeter. Since a thermal neutron capture imparts an average of 780 eV of energy to a silicon atom, the defects produced by recoil of the lattice atoms resulting from these captures was possibly the main source of degradation of the all-Boron-11 devices. Also, thermal neutron captures by the Boron-10 in the collector dopant may have made a significant contribution to the observable damage. Bulk displacement from Compton scatter of gamma rays probably also contributed to the damage observed in the 100 percent Boron-11 transistors.

## SECTION V

## CONCLUSIONS AND RECOMMENDATIONS

For each of the 42 transistors exposed to thermal neutron irradiation, the damage observed was proportional to the fraction of the emitter dopant atoms that were Boron-10. It is therefore concluded that the hypothesized source of thermal neutron damage (ref. 1) in bipolar PNP transistors is the main source of the thermal neutron damage observed in this experiment. Also, the thermal neutron fluence and current dependence of the gain degradation indicated that bulk displacement damage was the source of damage. It was also observed that for these transistors, where the combined width of the emitter and base regions is less than the path length of a 0.88 MeV lithium nucleus in silicon, the dependence of gain degradation on the width of the base region was roughly the same for fast and thermal neutrons. One-MeV neutrons were found to be approximately 20 times more effective than thermal neutrons in degrading the gain of the transistors with 100 percent Boron-10 emitter dopant atoms and 100 times more effective in degrading the transistor doped with 20 percent Boron-10 and 80 percent Boron-11. By applying a geometry factor that was developed, it was found that a 1-MeV neutron produces about 3.3 times as many defects in silicon as are produced by the average particle (lithium or alpha doing damage in the base). An equation was developed to permit the calculation of the relative sensitivity of a given transistor to thermal neutron damage.

Since much of the material in the environment can conceivably thermalize neutrons from nuclear weapons, and since the effectiveness of thermal neutrons in producing damage can be reduced by using 100 percent Boron-11 as the dopant material, it would be desirable to use 100 percent Boron-11 doped transistors in underground or underwater electronic systems that must function in a nuclear environment. However, since pure Boron-11 would be expensive, it may be more cost effective to use the relative damage equation developed to obtain device geometries more resistant to thermal neutron damage.



## APPENDIX A

A GENERAL PROOF OF THE  $\beta$  DEGRADATION EQUATION FOR BULK DISPLACEMENT DAMAGE

Copyright 1973 by the Institute of Electrical and Electronic Engineers, Inc.  
Reprinted, with permission, from IEEE Transactions on Nuclear Science (ref. 15).

## ABSTRACT

A general proof for the  $\beta$  degradation equation in displacement producing radiation environments is presented. The proof is straightforward for the base component of damage. An extension of the proof encompasses damage in the base emitter field region to the extent it can be related to the emitter time constant. The derivation assumes a significant post-radiation common emitter current gain ( $\beta > 3$ ).

The relationship between common-emitter current gain and displacement damage has been given as<sup>(1)</sup>

$$\frac{1}{\beta} = \frac{1}{\beta_1} + \frac{\phi}{\omega_T K} \quad (1)$$

where  $\beta$  is common-emitter current gain,  $\beta_1$  is the initial unirradiated value of common-emitter current gain,  $\omega_T$  is  $2\pi$  times the common emitter gain bandwidth product,  $\phi$  is the damaging radiation fluence and  $K$  is the relevant lifetime damage constant. This relationship was initially proven for homogeneous base transistors and later extended to cover exponentially graded base transistors<sup>(2)</sup>. The following proof will show that this relationship is true for any base doping profile as long as the transistor retains a significant common-emitter current gain ( $\beta > 3$ ).

Gover<sup>(3)</sup> has shown that for any arbitrary base impurity distribution, the series expansion for the base transport factor is

$$\alpha = 1 - U_1 \frac{W^2}{L^2} + U_2 \frac{W^4}{L^4} - \dots \quad (2)$$

where  $\alpha$  is the base transport factor,  $W$  is the base width and  $L = \sqrt{D\tau}$  is the diffusion length. The coefficients  $U_1$ ,  $U_2$  etc., are determined by successive iteration of the equation pair.

$$n(X) = -\frac{1}{qN} \int_X^{X_2} \frac{N}{D} J dX \quad (3)$$

$$J(X) = J^0 + q \int_{X_1}^{X_2} \frac{n}{\tau} dX$$

where  $n$  is the excess minority carrier concentration in the base,  $N$  is the impurity density in the base,  $D$  is diffusion constant,  $\tau$  is minority carrier lifetime,  $q$  is electron charge, and  $J$  is minority current density.

Specifically, this procedure leads to the following deterministic equations for  $U_1$  and  $U_2$ :

$$U_1 = \frac{D(X_2) \tau(X_2)}{W^2} \int_{X_1}^{X_2} \frac{dX}{\tau(X) N(X)} \int_X^{X_2} \frac{N(\bar{X}) d\bar{X}}{D(\bar{X})} \quad (4)$$

$$U_2 = \frac{D^2(X_2) \tau^2(X_2)}{W^4} \int_{X_1}^{X_2} \frac{dX}{\tau(X) N(X)} \int_X^{X_2} \frac{N(\bar{X}) d\bar{X}}{D(\bar{X})}$$

$$\int_{X_1}^{\bar{X}} \frac{d\bar{X}}{\tau(\bar{X}) N(\bar{X})} \int_{\bar{X}}^{X_2} \frac{N(\bar{X}) d\bar{X}}{D(\bar{X})}$$

A recombination series corresponding to Equation (2) exists for  $n$  and  $j$ .

$$J(X) = J^0(X) + J^1(X) + \dots$$

$$n(X) = n^0(X) + n^1(X) + \dots \quad (5)$$

Now,

$$1 - \alpha = -\frac{(J^1 + J^2 + J^3 + \dots)}{J^0} = -\frac{J^1}{J^0} \quad (6)$$

The series expansion is rapidly convergent and can be terminated at  $J^1$  since

$$U_2 \frac{W^4}{L^4} \ll U_1 \frac{W^2}{L^2} \quad \text{except for transistors so seriously}$$

damaged that they are no longer of practical interest.

From Equation (2) and assuming that base transport is the dominant factor in the radiation dependence of common emitter current gain

$$\frac{1}{\beta} = \frac{U_1 W^2}{D \tau} \quad (7)$$

Gover<sup>(3)</sup> also shows that when  $n/\tau$  is described by a single time constant, i. e.,

$$\frac{1}{q} \frac{\partial J}{\partial X} = \frac{n}{\tau} (1 + j\omega\tau), \quad \omega_T = \frac{D}{U_1 W^2} \quad (8)$$

again truncating the recombination series at the first-order term.

Now minority carrier lifetime as a function of displacement fluence is given by

$$\frac{1}{\tau} = \frac{1}{\tau_1} + \frac{\phi}{K} \quad (9)$$

15. Messenger, George C., "A General Proof of the Degradation Equation for Bulk Displacement Damage," IEEE Transactions on Nuclear Science, NS-20 1, February 1973.

for all damaging radiations including neutrons, protons, electrons and  $\gamma$  rays with the appropriate choice of  $K$ .

Combining this result with Equation (7) gives

$$\frac{1}{\beta} = \frac{1}{\beta_1} + \frac{U_1 W^2}{D} \frac{\phi}{K} \quad (10)$$

Note that  $\frac{1}{\beta_1}$  may also contain a surface recombination, and an emitter efficiency contribution as long as they do not change significantly with displacement fluence.

Combining this result with Equation (8) gives

$$\frac{1}{\beta} = \frac{1}{\beta_1} + \frac{\phi}{\omega_T K} \quad \text{Q. E. D.} \quad (11)$$

The base impurity distribution is arbitrary, both  $\tau$  and  $D$  may be functions of  $X$ , but the transistor must have significant common-emitter current gain, i. e.,

$$U_2 \frac{W^4}{L^4} \ll U_1 \frac{W^2}{L^2}$$

Values of  $U_1$  and  $U_2$  are given in Table 1 for homogeneous and exponential impurity distributions. The error function impurity distribution produces  $U_1$  and  $U_2$  values very similar to the exponential distribution.

Homogeneous Base		Exponential Base
$N = \text{Const.}$		$N = N_0 e^{-\eta X/W}$
$U_1$	$\frac{1}{2}$	$\frac{\eta + e^{-\eta} - 1}{\eta^2}$
$U_2$	$\frac{5}{24}$	$\frac{1}{2} \eta^2 - 2 + (3\eta + 1)e^{-\eta} + e^{-2\eta}$
		$\eta^4$

Table 1

Values of  $U_1$  and  $U_2$  for Homogeneous and Exponential Impurity Distribution with  $D$  and  $\tau$  constant.

Ramsey and Vail<sup>(4)</sup> have shown that the emitter efficiency contribution resulting from recombination in the emitter base field region can be related to the emitter time

constant,  $\tau_e C_e$ . Equation (9) strictly relates to the cut-off frequency for base transport; it can be readily extended to include the emitter time constant.

$$\omega_T = \left( \tau_e C_e + \frac{U_1 W^2}{D} \right)^{-1} \quad (12)$$

Including both emitter-base field recombination and base recombination and extending Equation (7) including the Ramsey and Vail<sup>(4)</sup> relationships.

$$\frac{1}{\beta} = \frac{U_1 W^2}{D\tau} + \frac{1}{\beta_1} = \frac{1}{\tau} \left( \tau_e C_e + \frac{U_1 W^2}{D} \right) \quad (13)$$

Combining Equations (12), (13) and (9) yields

$$\frac{1}{\beta} = \frac{1}{\beta_1} + \frac{\phi}{\omega_T K} \quad \text{Q. E. D.} \quad (14)$$

This extends the proof to cover both emitter-base field recombination and bulk recombination subject to the additional approximations used by Ramsey and Vail<sup>(4)</sup> to obtain Equation (13).

#### References

- (1) Messenger, G. C. and Spratt, J. P. "The Effects of Neutron Irradiation on Germanium and Silicon," New York Meeting of Electrochemical Society, April 1958. Published in Proceedings IRE, June 1958, pp 1038-1044.
- (2) Messenger, G. C. "Current Gain Degradation due to Displacement Damage for Graded Base Transistors," Proc. IEEE Vol. 55 No. 3, March 1967, pp 160.
- (3) Gover, et al "Bipolar Transistor Base Parameters and Impurities," PGED-19 Vol. 8, August 1972, pp 967-975.
- (4) C. Ramsey and P. Vail "Current Dependence of the Neutron Damage Factor," PGNS Vol. NS-17 No. 6, pp 310-135.

APPENDIX B  
GEOMETRY FACTOR CALCULATION

The geometry factor is the portion of particles produced in the emitter that do all of their damage in the base region. This calculation of the geometry factor requires the following assumptions:

1. All directions of particle emission are equally probable.
2. The path length of the particles is short compared to the surface area of the devices.
3. The range of the particle is greater than the thickness of the emitter and base regions.
4. The particle does all of its displacement damage at the end of its path length.

Then the locus of points at which a particle originating at a given location can do damage would form a sphere of radius equal to the range of the particle, with its center at the point of origin. By assumption 3, the sphere must contain a complete thickness of the slab of the base region (figure 17).

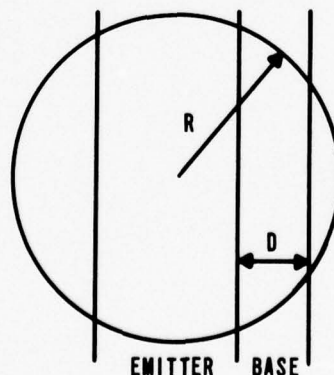


Figure 17. Geometry Factor Relationships



Let the range of the particle be  $R$  and the thickness of the base region be  $D$ . Then the area  $S$  of the intersection of the sphere with the base region is just

$$S = 2 \pi R D$$

This is true, regardless of the position of the slab in the sphere, as long as a complete base region width is contained in the sphere as required by assumption 3. The total area of the sphere  $A$  is

$$A = 4 \pi R^2$$

Since  $A$  is a measure of all possible damage sites and  $S$  is a measure of those in the base region, the fraction produced that ends in the base region is just  $S/A$  or

$$G = \frac{D}{2R}$$

where  $G$  is the fraction of total particles produced that do damage in the base region. Note that the distribution of sources across the emitter region is unimportant as long as assumptions 1 through 4 are met.

## APPENDIX C

## THERMAL NEUTRON REACTION RATE IN PNP TRANSISTORS

The  $B^{10} (n, \alpha) Li^7$  reaction is exothermic with an energy release of 2.78 MeV. In reactions involving thermal neutrons, the probability of forming  $Li^7$  in the ground state is only 0.064. Instead, an intermediate excited state of  $Li^7$  is formed, followed by the emission of a 0.48 MeV gamma ray. Thus, the total kinetic energy available to the  $Li^7$  nucleus and the alpha is as follows

$$E_{Li} = \frac{E_{KE} M_{\alpha}}{M_{\alpha} + M_{Li}} = \frac{(2.30)(4.00)}{(4.00) + (7.02)} = 0.83 \text{ MeV} \quad (1)$$

$$E_{\alpha} = \frac{E_{KE} M_{Li}}{M_{Li} + M_{\alpha}} = 1.47 \text{ MeV} \quad (2)$$

Up to 30 keV, the cross section ( $\sigma$ ) for this reaction has a  $1/v$  dependence, where  $v$  is the thermal neutron velocity. This can be represented as follows

$$\sigma = \frac{\sigma_0 v_0}{v} \quad (3)$$

where  $v_0 = 2.2 \times 10^5$  cm/sec and  $\sigma_0 = 3840$  barns  $= 3.84 \times 10^{-21}$  cm<sup>2</sup>.

This  $1/v$  dependence can be used to calculate the reaction rate,  $dR$ , resulting from neutrons with energies between  $E$  and  $E + dE$  in the volume element  $dV$

$$dR = N(x, y, z) \sigma(E) \phi(E, x, y, z) dE dV \quad (4)$$

where  $N(x, y, z)$  = the number of  $B^{10}$  atoms per unit volume at the point  $(x, y, z)$ ;  $\sigma(E)$  = the  $B^{10} (n, \alpha)$  cross section at energy  $E$  corresponding to the velocity  $V$  through the equation  $E = \frac{1}{2} m_n v^2$ ; and  $\phi(E, x, y, z)$  = the flux per unit energy interval at the point  $(x, y, z)$ . Since the flux is, for these purposes, assumed to be independent of position, write

$$\phi(E, x, y, z) = \phi(E) \quad (5)$$

Write

$$\phi(E) = n(E)v \quad (6)$$

where  $n(E)$  is the number of thermal neutrons per unit volume per unit energy interval with energies between  $E$  and  $E + dE$ . Combining equations 3 and 6,

$$\phi(E) \sigma(E) = [n(E)v] \left[ \sigma_0 v_0 / v \right] = n(E) \sigma_0 v_0 \quad (7)$$

The resulting expression for  $dR$  is thus

$$dR = N(x,y,z) n(E) \sigma_0 v_0 dE dV \quad (8)$$

This may be integrated to yield the total number of reactions,  $R$ , produced by an arbitrary spectrum of neutrons with energies below 30 keV

$$R = \sigma_0 v_0 \int_{V_0} \int_0^{30 \text{ keV}} N(x,y,z) n(E) dE dV = \sigma_0 v_0 \int_{V_0} N(x,y,z) dV \int_0^{30 \text{ keV}} n(E) dE \quad (9)$$

Here

$$\int_{V_0} N(x,y,z) dV = N_B \quad (10)$$

where  $N_B$  = total number of Boron-10 atoms in sample, and

$$\int_0^{30 \text{ keV}} n(E) dE = n \quad (11)$$

where  $n$  is the number of neutrons per unit volume, irrespective of energy up to 30 keV incident on the sample.

Thus

$$R = N_B \sigma_0 v_0 n \quad (12)$$

Note that equation 12 is independent of both the neutron spectrum and of the distribution of the boron atoms in the sample. Equation 12 can be expressed in terms of the neutron flux,  $\phi = n \bar{v}$ , where  $\bar{v}$  is the average neutron velocity



$$R = \frac{N_B \sigma_0 v_0 \phi}{\bar{v}} \quad (13)$$

For a Maxwell-Boltzman distribution in thermal neutron energy,  $\bar{v}$  is  $1.128 v_0$  at  $20^\circ \text{C}$ . For this spectrum

$$R = \frac{N_B \sigma_0 \phi}{1.128} \quad (14)$$

This equation can also be expressed in terms of the total neutron fluence,  $\phi$ , incident on the sample in time  $t$ . Here assume that the neutrons are deposited uniformly in time and write

$$\phi = \phi t \quad (15)$$

Thus, write

$$R = \frac{N_B \sigma_0 \phi}{(1.128)t} \quad (16)$$

The total number,  $N$ , of alphas produced is

$$N_\alpha = Rt = \frac{N_B \sigma_0 \phi}{(1.128)} \quad (17)$$

or since  $\sigma_0 = 3.84 \times 10^{-21} \text{ cm}^2$  (ref. 16)

$$N_\alpha = (3.4 \times 10^{-21} \text{ cm}^2) N_B \phi \quad (18)$$

Note that only 18.45 to 18.98 percent of naturally occurring boron is  $B^{10}$ . The bulk of naturally occurring boron is  $B^{11}$ .

Now consider a specific example of a PNP bipolar transistor whose emitter is heavily doped with boron. Typical dopant concentrations at the junction between the emitter and the base are  $10^{20}$  boron atoms per  $\text{cm}^3$ . Also assume that this transistor is irradiated by thermal neutrons with a Maxwell-Boltzman

---

16. Hughes, Donald J. and Robert B. Schwartz, Neutron Cross Sections, BNL 325, Brookhaven National Laboratory Associated Universities, Upton, Long Island, New York, 1 July 1958.

spectrum to a fluence of  $5 \times 10^{11}$  n/cm<sup>2</sup>. Further, assume that the PNP transistor is of planar construction, with a base width of 0.7 microns and an emitter width of 1.3 microns. Since the range of an alpha particle from the  $B^{10}(n,\alpha)Li^7$  reaction is 10 microns, the alpha penetrates far into the collector where most of its energy is dissipated. Assume also that the emitter is 1 mil by 1.5 mils in area. Since there are 25.4 microns to a mil, these dimensions are large compared to the range of the alpha. Thus, calculate by use of equation 18 the total number of boron ( $n,\alpha$ ) reactions which occur.

$$\begin{aligned}
 N_{\alpha} &= (3.4 \times 10^{-21} \text{ cm}^2) \phi N_B \\
 &= (1.7 \times 10^{-9}) N_B \\
 &= (1.7 \times 10^{-9}) \left( 10^{20} \frac{B}{\text{cm}^3} \right) (2.5 \times 10^{-3} \text{ cm}) \times \\
 &\quad (3.75 \times 10^{-3} \text{ cm}) (1.3 \times 10^{-4} \text{ cm}) (.1898 B^{10}/B) \\
 N_{\alpha} &= 39.3 \text{ alphas} = N_{Li} = 39.3 Li^7 \text{ atoms}
 \end{aligned} \tag{19}$$

Since half of these alphas are directed toward the surface, the result is that there are only 20 which penetrate the base region. Since this is such a small number of alphas, any damage or ionization produced may be neglected. For example, assume for a worst case ionization condition that all of the energy of the alpha and the lithium recoil atom goes into ionization. The result will be no more than a thousand rads silicon deposited in the transistor even when the short range of the lithium recoil is considered in a calculation of effective collection volume. Note that a rad is an expression of energy per gram, and as the collection volume decreases, the rads deposited will increase in this case. Increasing the emitter area does not have any effect on the rads deposited for this same reason. It is also easy to see that the damage due to 20 alphas and 20  $Li^7$  nuclei will also be negligible. Increasing the area also has no effect on the ratio of damage to area, which determines the degradation. Only an increase of doping level and emitter thickness to unrealistic dimensions will yield enough alphas to degrade the transistor.

APPENDIX D

NBS-2 TEST PATTERN

Note: All dimensions in mils. Center of mask is taken as (0,0); horizontal coordinate is given first followed by vertical coordinate. One square equals  $\frac{1}{4}$  mil. Lines not on grid lines are halfway between grid lines. C = Center. R = Radius. S = Distance from C to one side of square.



Table 3  
TEST STRUCTURES  
(Numbers Refer to Figure 18)

Number	Test Structure	Dimension,* mil
1	Gated circular base-collector junction with diffused channel stop	D = 6
2	Ungated circular base-collector junction with diffused channel stop	D = 6
3	Ungated square base-collector junction with diffused channel stop	S' = 5
4	Gated square base-collector junction with diffused channel stop	S' = 18
5	Ungated circular base-collector junction with diffused channel stop	D = 20
6	Gated circular base-collector junction with diffused channel stop	D = 20
7	Gated circular base-collector junction (small emitter) with diffused channel stop	D = 20
8	Gated circular base-collector junction (large emitter) with diffused channel stop	D = 20
9	Gated circular base-collector junction with diffused channel stop	D = 60
10	MOS capacitor over collector with field plate and diffused channel stop	D = 6
11	MOS capacitor over collector with field plate and diffused channel stop	D = 20
12	MOS capacitor over collector with distant field plate and diffused channel stop	D = 20
13	MOS capacitor over base without field plate and diffused channel stop	D = 20
14	Base sheet resistor	
15	Emitter sheet resistor	
16	Metal-to-base contact resistor	
17	Metal-to-emitter contact resistor	
18	Collector resistor	
19	Base-under-the-emitter sheet resistor (tetrode transistor)	
20	Hall effect pattern	
21	Alignment marker	

\* D = diameter of a circle, S' = side of a square. Tolerances should be held to  $\pm 0.1$  mil. If metric dimensions are desired, the diameters should be 0.15 mm (for structures numbered 1, 2, 10), 0.5 mm (5-8, 11-13), and 1.5 mm (9); and the sides should be 0.13 mm (3) and 0.46 mm (4); all tolerances should be held to  $\pm 0.002$  mm.

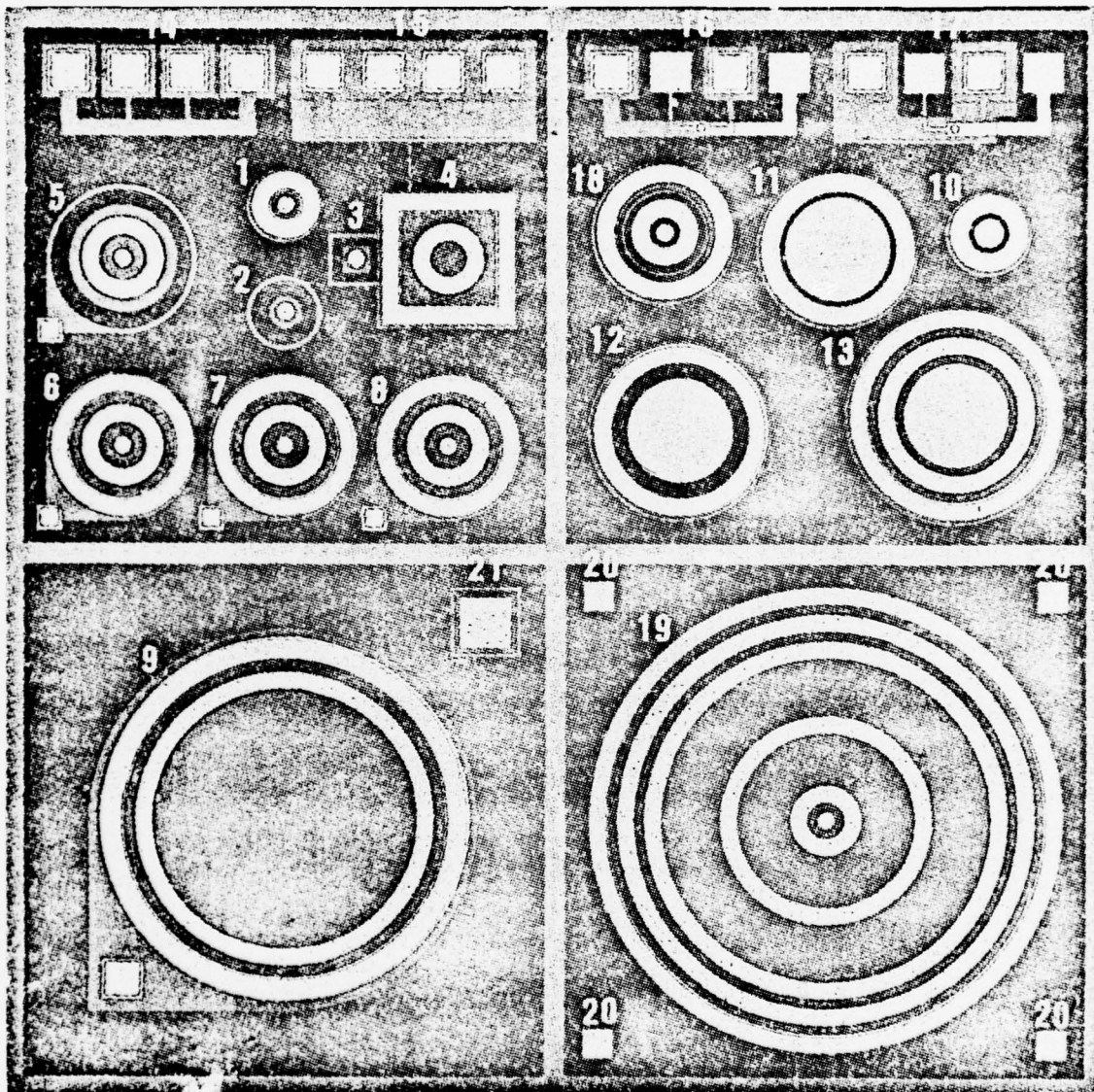


Figure 18. Test Pattern, NBS-2, for Characterizing the Electrical Properties of Silicon MOS Capacitors and p-n Junctions. (The 21 elements are identified in table 3. The overall pattern is 200 mil [5.08 mm] on a side.)

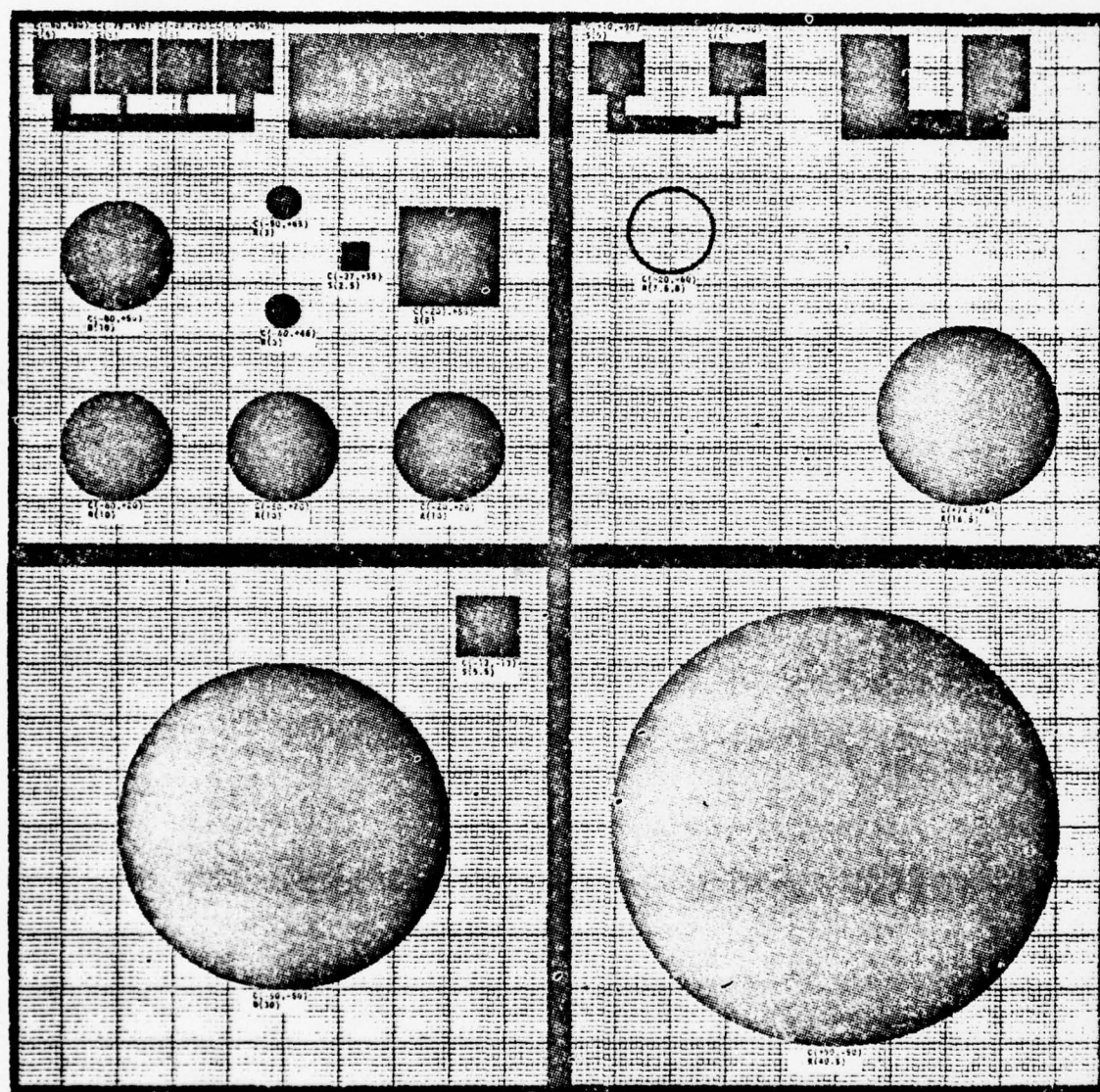


Figure 19. Base Mask

(For positive photoresist, black areas are clear on final mask.)



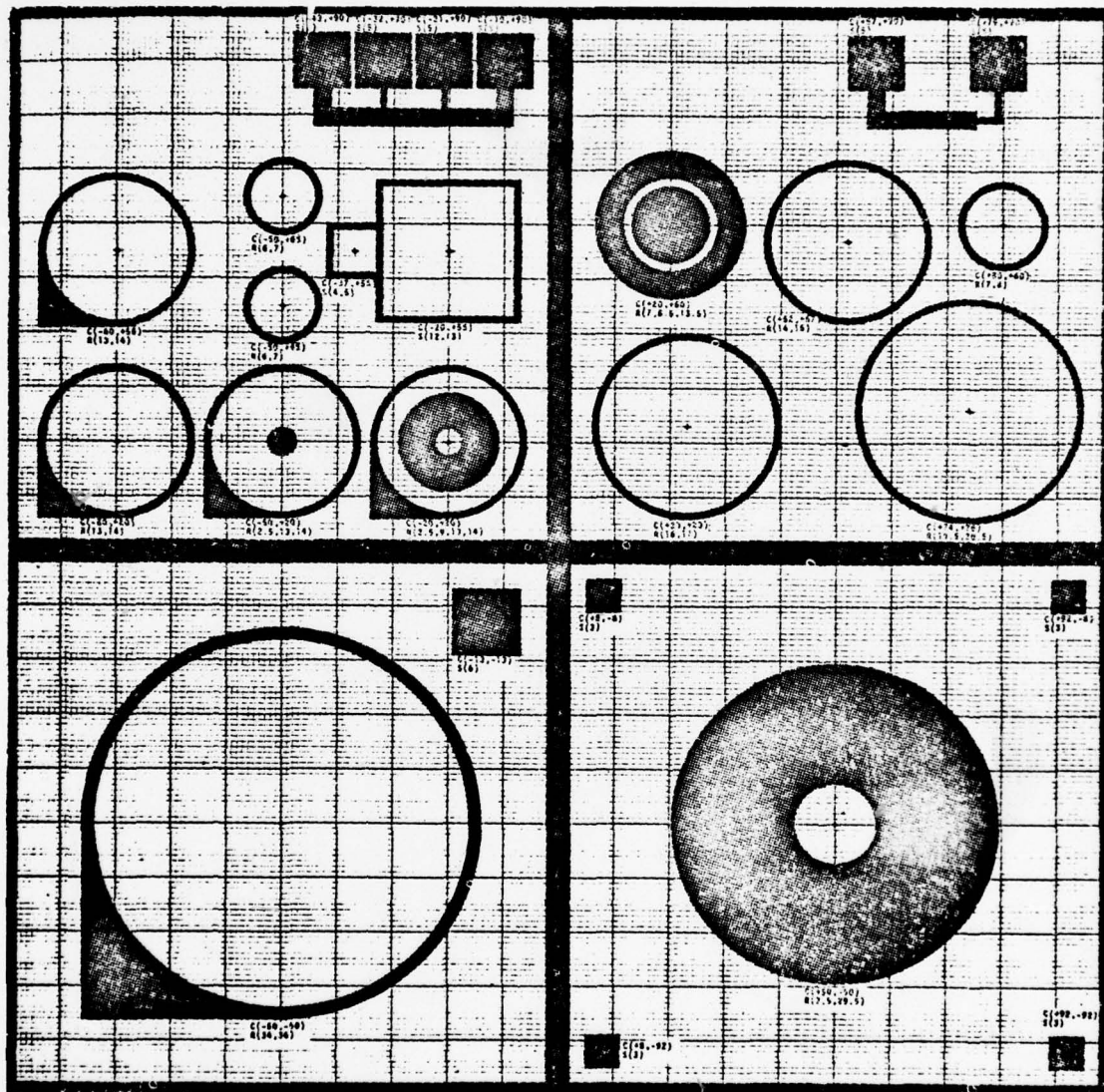


Figure 20. Emitter Mask

(For positive photoresist, black areas are clear on final mask.)

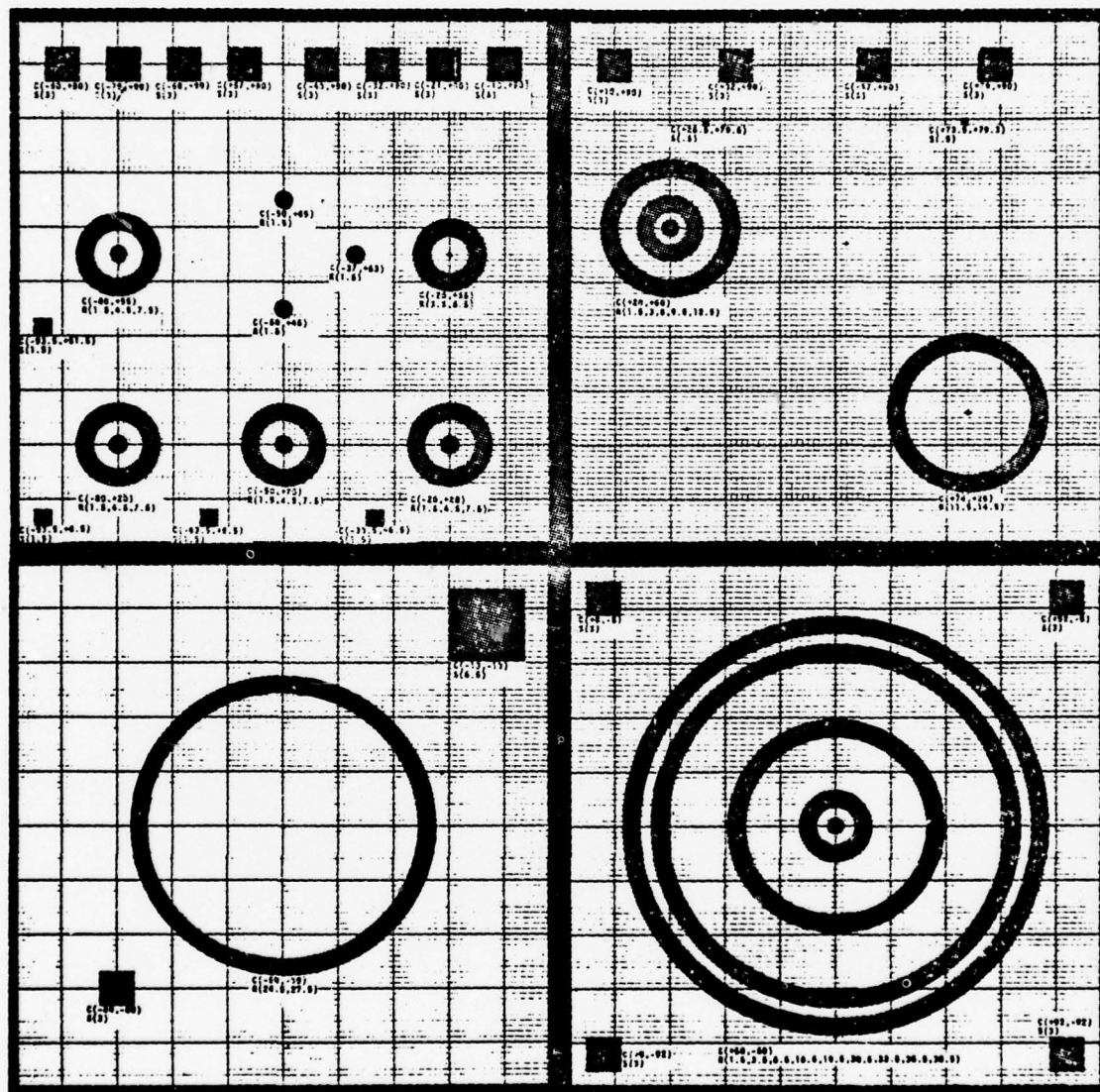


Figure 21. Contact Mask

(For positive photoresist, black areas are clear on final mask.)

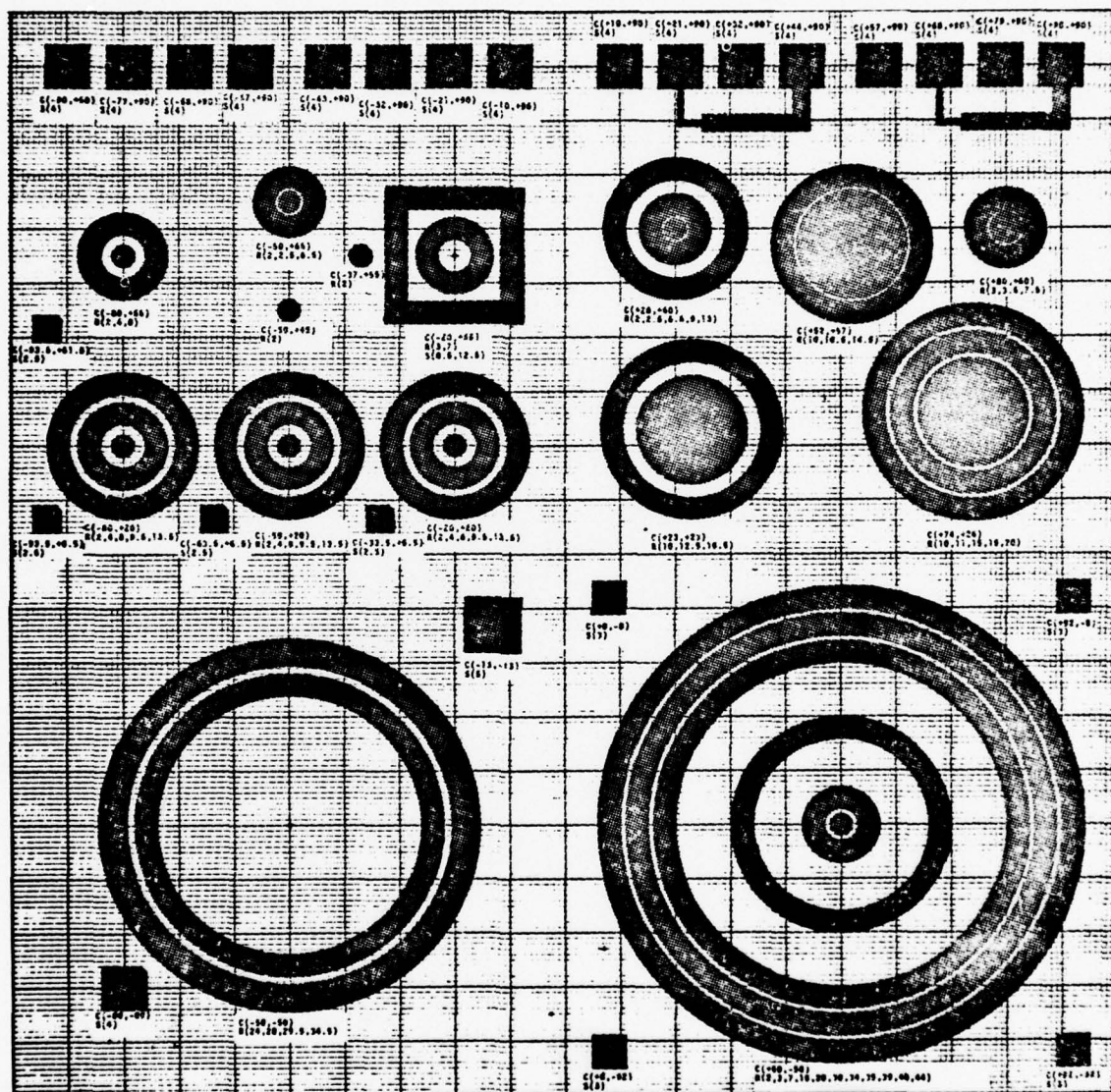


Figure 22. Metal Mask

(For positive photoresist, black areas are black on final mask.)



APPENDIX E  
TRANSISTOR PROCESS INFORMATION

# CONTROL WAFER MEASUREMENTS

- C1 - Base Implant, drive-in A      Drive-in B: we,4,2,8,4,12  
      Rs = 193  $\Omega/\square$       Drive-in A: w1,2,5,6,9,10  
      Xj = 1.55  $\mu\text{m}$
- C2 -  $^{11}\text{B}$  Emitter + base, drive-in A  
      Rs = 24.8  $\Omega/\square$   
      Xj = 1.05  $\mu\text{m}$
- C3 -  $^{11}\text{B}$  Emitter + base, drive-in B  
      Rs = 24.6  $\Omega/\square$   
      Xj = 1.09  $\mu\text{m}$
- C4 -  $^{10}\text{B}$  Emitter + base, drive-in A  
      Rs = 25.0  $\Omega/\square$   
      Xj = 0.90  $\mu\text{m}$
- C5 - 80%  $^{11}\text{B}$  + 20%  $^{10}\text{B}$  emitter + base, drive-in A  
      Rs = 25.3  $\Omega/\square$   
      Xj = 0.93  $\mu\text{m}$

---

For Base:  $\bar{\sigma} = \frac{1}{R_s X_j} = 33.4 (\Omega\text{-cm})^{-1}$

from Irvin's Curves    Cs  $\approx 2 \times 10^{18} \text{ cm}^{-3}$  (for  $10^{12}$  substrate)  
      (Gaussian)

For Emitter:  $\bar{\sigma} = \frac{1}{R_s X_j} \approx 400 (\Omega\text{-cm})^{-1}$

from Irvin's Curves    Cs  $\approx 10^{20} \text{ cm}^{-3}$  (for  $10^{12}$  substrate)  
      (Gaussian)

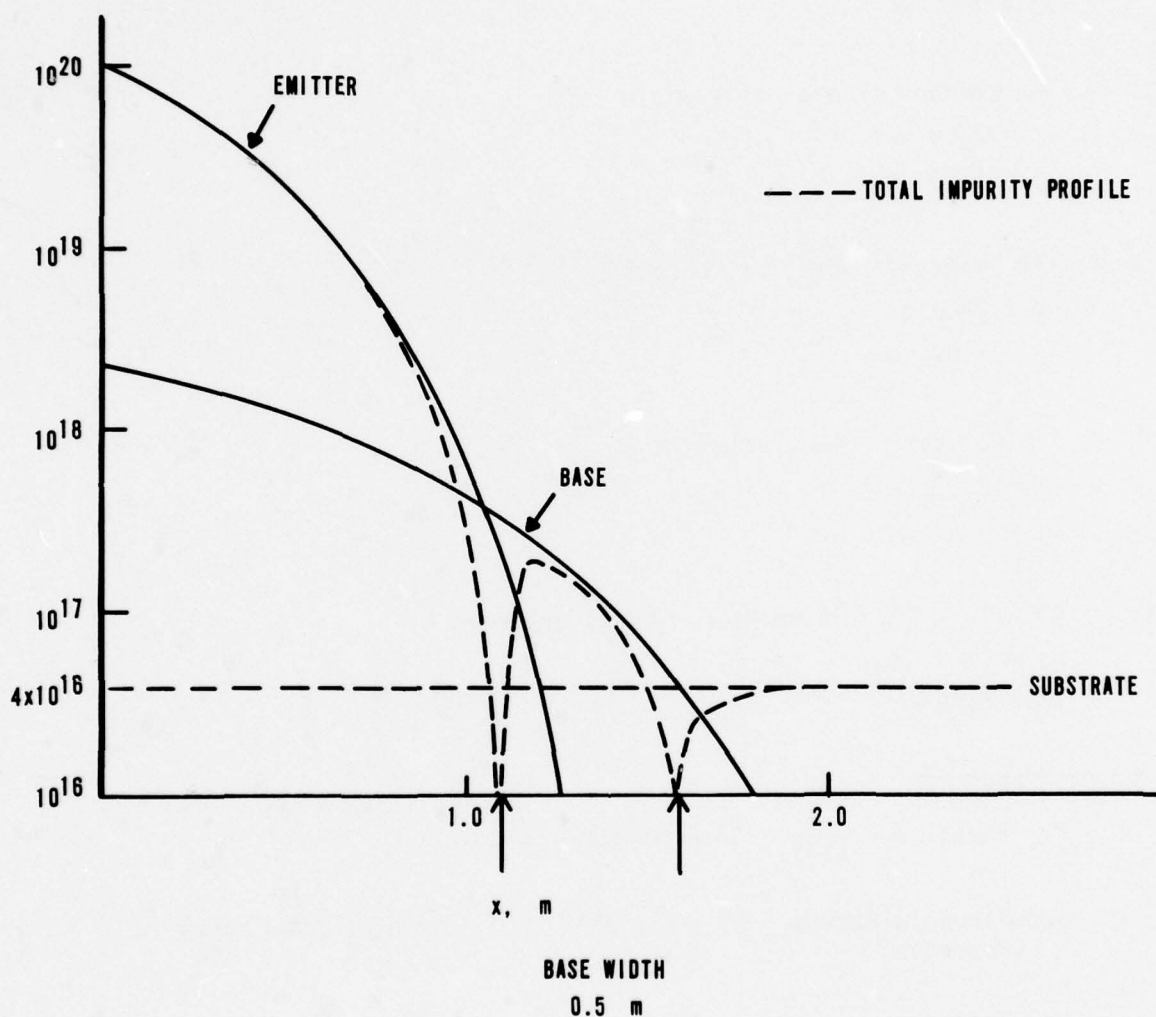


Figure 23. Doping Profile; Approximate Impurity Profiles Based on Gaussian Profiles Using Irvin's Curves. (These curves are hand-down fits through  $C_s$  and  $X_j$  points, so are merely representations of actual profiles.)

# PACKAGED DEVICE PIN CONNECTIONS

Notation: Each can has a number scratched on the lid.

4A - Devices from wafer 4, chip A

[Chip A contains small transistor (structure #7) and emitter resistor (structure #15).]

4B - Devices from wafer 4, chip B

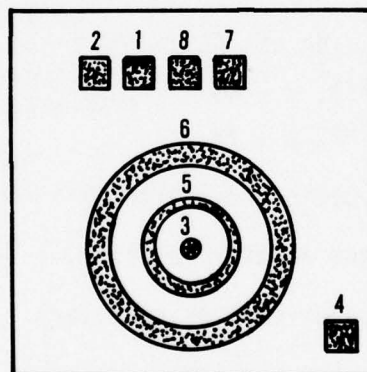
[Chip B contains structure #19, tetrode transistor.]

similarly for others such as

2A, 2B, 6A, 6B, etc. In each case the number refers to the wafer number.  
See process sequence.

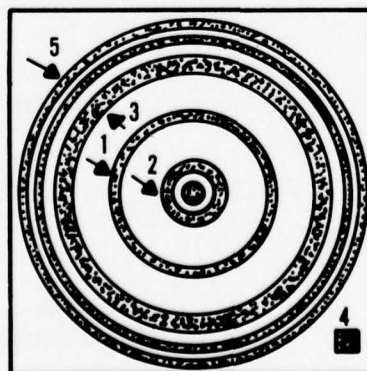
## PIN CONNECTIONS

CHIP A



PIN 6 IS FIELD PLATE  
AT COLLECTOR-BASE JUNCTION

CHIP B

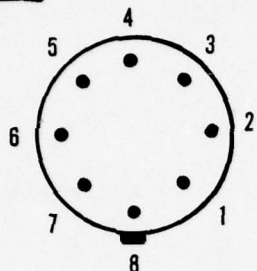


PIN 5 IS FIELD PLATE AT  
COLLECTOR BASE JUNCTION

PINS 3 & 2 ARE BASE CONTACTS



TO-5 HEADERS



Top View pin numbering.  
Pin 4 is shorted to header, thus  
is used for collector.

Each can lid has number identifying wafer and type of chip contained therein.  
Wafer numbers refer to processing sequence.

Wafer Numbers: 2 -  $^{11}\text{B}$  emitter,  $\beta \sim 40$   
4 -  $^{11}\text{B}$  emitter,  $\beta \sim 75$   
6 -  $^{10}\text{B}$  emitter,  $\beta \sim 40$   
8 -  $^{10}\text{B}$  emitter,  $\beta \sim 75$   
10 - 0.8  $^{11}\text{B}$  + 0.2  $^{10}\text{B}$ ,  $\beta \sim 40$   
12 - 0.8  $^{11}\text{B}$  + 0.2  $^{10}\text{B}$ ,  $\beta \sim 75$

Note that  $\beta$  may vary somewhat from device to device.

Chip A: Small emitter transistor and emitter resistor.

Chip B: Tetrode transistor (base-under-emitter resistor).

## PROCESS SEQUENCE FOR D0301A BIPOLAR TRANSISTORS

Wafers are P-Boron (100) 0.4 - 0.6  $\Omega$ -cm  
NBS-2 Mask Set

12 Active  
5 Controls

1. Acid Clean	A + C
2. Dry/Steam Oxide; 15/90 min, 1100° C	A + C
3. Neg PR, lev 1 (base)	A
4. BOE Etch	A + C
5. Clean (PR strip)	A
6. Phos Implant; $1.3 \times 10^{14}$ at 160 keV	A + C
7. Etch 4 min ( $\sim 4000\text{\AA}$ )	A + C
8. Base drive-in, Dry $O_2$ , 1100° C, 120 min	A + C
9. Neg PR, lev 2 (emitter)	A
10. Etch	A + C2-C5
11. Boron Implant; $^{11}\text{B} + 5 \times 10^{15}$ at 60 keV	W 1-4, C2, C3
12. Boron Implant; $^{10}\text{B} + 5 \times 10^{15}$ at 60 keV	W 5-8, C4
13. Boron Implant; 80% $^{11}\text{B} + 20\% ^{10}\text{B} + 5 \times 10^{15}$ , 60 keV	W 9-12, C5
14. Clean (PR strip)	A
15. Deposit 5 x $\text{\AA}$ oxide	A + C
16. Emitter drive-in; 1000° C, 30 min, $N_2$	A + C
17. Emitter drive-in; 1000° C, 30 min, $N_2$	W3,4,7,8,11,12,C3
18. Neg PR, lev 3 (contact)	A
19. Etch	A + C
20. Clean (PR strip)	A
21. Probe wafer-gain measurement	
22. Clean	
23. Drive-in; 1100° C, 15 min, $N_2$	W1, 3
24. 30 sec Etch	W1, 3
25. Probe wafer	
26. Drive-in; 1100° C, 12 min, $N_2$	A + C except W1, 3
27. 15 sec Etch	A + C except W1, 3
28. Probe wafer	
29. Clean	A + C
30. Drive-in; 1000° C, 30 min, $N_2$	A + C except W1, 3
31. 15 sec Etch	A + C except W1, 3
32. Al Evap, 10K $\text{\AA}$	A
33. Neg PR, lev 4 (metal)	A
34. Etch Al	A
35. PR strip	A
36. Sinter, 5% forming gas, 450° C, 20 min	A
37. Scribe, die attach, bond	

Notes: A means active wafers.  
C means control wafers.

DEVICE NUMBER-- D03010

DEVICE DESCRIPTION IS BIPOLAR TRANSISTOR AND WAS DEFINED 07/13/76  
BY ANDERSON AND ENTERED BY TUCK

FOR 17 WAFERS

REMARKS WAFERS ARE P-BORON (100) 0.4-6.5; 12 ACTIVE + 5 CONTROLS; NBS/2 MASK SET

OPN	NO	NUMBER	PROCESS DESCRIPTION	OPTR INIT	COMPLETION TIME	DATE	NUMBER WAFERS	NOTES
	1	1106CC	CLEAN	MRT	13:51	7/14/76	17	0
	2	3102HB	D/S OX 8000ACC	EH	15:58	7/14/76	17	17
	3	5100BB	747/60, LEV, L 3.55	MRT	9:50	7/15/76	12	0
	4	5111AH	ETCH HYP0 + 1 MIN	MRT	10:10	7/15/76	17	* 0
	5	1100AA	CLEAN	DLW	11:24	7/15/76	17	0
	6	4134PV	PHOS IMP. A+C	REB	14: 1	7/15/76	17	0
	7	5111BB	ETCH 4 MIN	MRT	8:31	7/16/76	17	0
	8	3107EF	BASE DRIVEIN, A+C1, CMRT		10:49	7/16/76	17	17
	9	5100EC	747/60, LEV-2, 3.58	MRT	16:14	7/16/76	12	* 0
	10	4505BH	BORON IMP, H+C, NOTE 1	REB	9:34	7/20/76	17	0
	11	1100AR	CLEAN	MRT	10:49	7/20/76	17	* 0
	12	2104AA	DEP. OX SKA, FRNTS A+CMRT		15: 4	7/20/76	17	0
	13	3110EB	DRINEIN, A+C	MRT	9: 0	7/21/76	17	13
	14	3110EB	W3, 4, 7, 8, 11, 12, C3	MRT	9:40	7/21/76	17	13
	15	5100AA	747/60, KEY 3, 0.55	MRT	10:57	7/21/76	17	0
	16	5111AA	ETCH HPO(C1) A+C	MRT	12:47	7/21/76	17	* 0
	17	9999AA	HOLD, MODIFY ENG.	MRT	8:44	7/26/76	17	0
	18	1100AA	CLEAN	MRT	10:19	7/26/76	15	0
	19	3000NN	N2 ANNEAL 12M, 1100C	MRT	10:54	7/26/76	17	0
	20	5111BD	30SEC ETCH	MRT	11:12	7/26/76	15	0
	21	9999AA	HOLD, NOTIFY ENG.	MRT	15:26	7/26/76	15	* 0
	22	1100BB	CLEAN	MRT	11:40	7/28/76	17	0
	23	6104BB	AL EVAP, 10KA	MRT	13:18	7/28/76	12	0
	24	5105RM	HR 100, LEV 4, 215	MRT	15:36	7/28/76	12	0
	25	5113RA	AL ETCH	MRT	16: 2	7/28/76	12	0
	26	1109AA	1100 RESIST STRIP	MRT	9: 2	7/29/76	12	0
	27	3100BB	SINTER, 5K FRING GASMRT		9:32	7/29/76	12	12
**	28	9000AA	MEAS RS, MJ ALL CONTROLS		:	/ /		
	29	9999AA	HOLD, NOTIFY ENG.		:	/ /		

SP

REH

\*- 1 NOTE 1: W1-4; C2, C3 IMPLANT B11 W5-8, C4 IMPLANT B10  
 \*- 1 W9-12, C5 IMPLANT 20% B10, 60% B11  
 \*- 1 ETCH LINE 9 MIN  
 \*- 9 ETCH AFTER PR STEP A+02-05 CONTROLS HYP0 + 1MIN  
 \*- 11 WAFERS - TWO ACID CLEANS, HOT H2SO4, PLASMA STRIPPED (ACT. ONLY), SCRUB  
 \*- 16 ETCH TIME 6MIN  
 \*- 17 WAFERS #1, 3, - 1100AA CLEAN, 1100 C H2 15 MIN (T9), 30S BOE - AFTER STE  
 \*- 18 STEP #19 TUBE 9  
 \*- 21 HI TER STEP 21 WAFERS (EXCP 1, 3) SCRUBBED, ACID CLEAN AND ANNEALED T13, H2  
 \*- 21 H2, 1000 DEGREES C 30MIN  
 \*- 26 SHT. RES 01: T-217; C-193; B-201; L-207; R-201 N TYPE  
 \*- 26 C2: 1-24.3; C-24.0; B-23.9; L-24.8; R-24.8; P-TYPE;  
 \*- 26 C3: C-24.6; C4: C-25.0; C5: C-25.3; P-TYPE RES. UNIFORM ACROSS WAFERS  
 \*- 28 XJ C1 15519A C2/10538A C3/10916H C4/8999A C5/9271A CMB 7/29/76

APPENDIX F  
TRANSISTOR CHARACTERISTICS



Table 4

DC GAIN MEASUREMENTS ON THE TEST TRANSISTORS  
AVERAGE OF THREE DEVICES WITH STANDARD DEVIATION

$I_c$ ma Device	.01	.02	.05	.1	.2	.5	1	2	10	20
2A	13.5	14.1	16.2	17.7	19.3	21.5	23.2	24.6	28.3	29.7
	1.35	1.97	2.06	2.19	2.24	2.39	2.28	2.34	2.31	1.70
4A	26.0	28.0	31.2	33.8	36.3	39.4	41.6	44.5	49.9	51.1
	5.05	4.88	4.95	4.93	5.41	5.39	5.37	5.19	5.38	5.21
6A	13.6	15.5	16.9	17.6	20.0	21.9	23.6	24.9	28.5	30.0
	1.22	1.62	1.29	1.41	1.46	1.23	1.17	1.23	1.47	1.59
8A	20.3	22.8	26.5	29.1	31.6	35.4	37.7	40.6	45.7	47.6
	2.51	2.24	2.17	2.12	1.97	1.53	1.73	1.68	2.00	1.60
10A	16.9	18.5	20.7	22.4	24.2	26.3	28.0	29.3	33.5	34.7
	1.30	1.15	1.26	1.11	1.16	1.16	1.50	1.29	1.44	1.32
12A	25.7	28.3	31.4	34.4	36.6	40.0	42.4	44.8	50.1	51.3
	5.08	4.89	4.85	5.49	5.20	5.34	5.51	5.46	5.91	5.95
2B							22.8	23.4	26.5	28.0
							2.92	2.05	1.32	1.17
4B							30.1	33.1	41.8	46.0
							4.58	3.67	6.93	.907
6B							22.7	24.6	29.9	32.3
							5.75	4.82	37.7	3.45
8B							41.9	39.4	43.5	47.0
							4.45	4.06	4.82	5.53
10B							19.8	21.7	26.5	28.5
							1.91	1.56	1.48	1.41
12B							29.2	32.3	40.8	45.0
							7.50	6.30	4.29	3.10

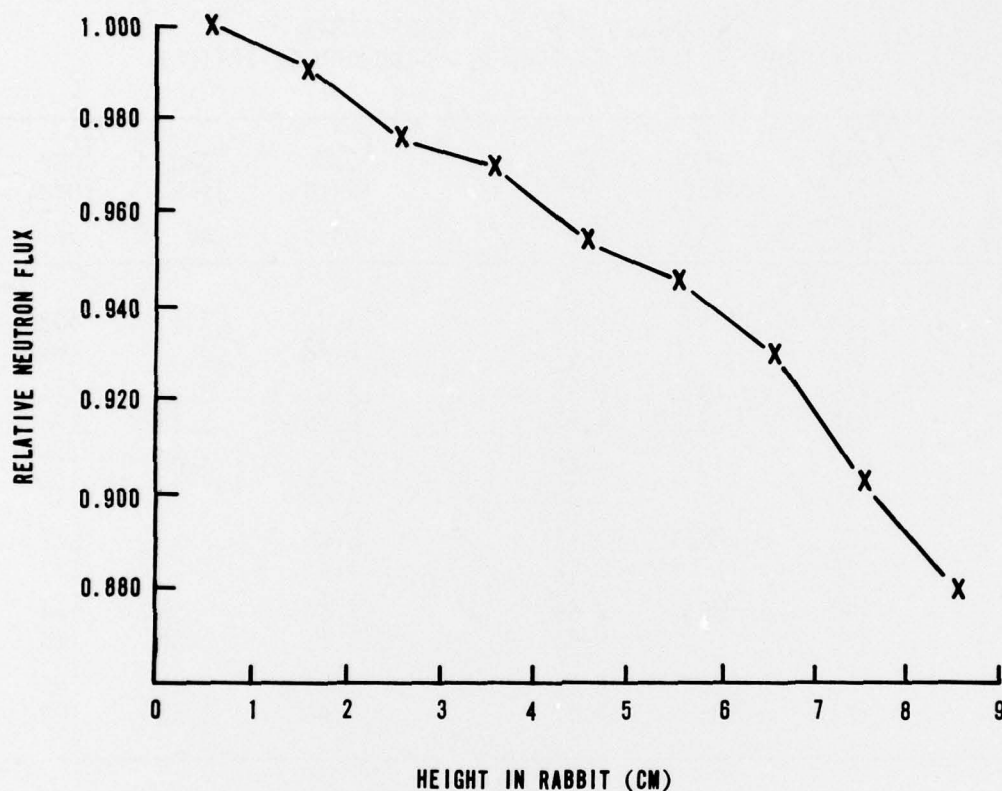
Table 5

LEAKAGES FOR TEST TRANSISTORS  
AVERAGE OF THREE DEVICES AND STANDARD DEVIATION

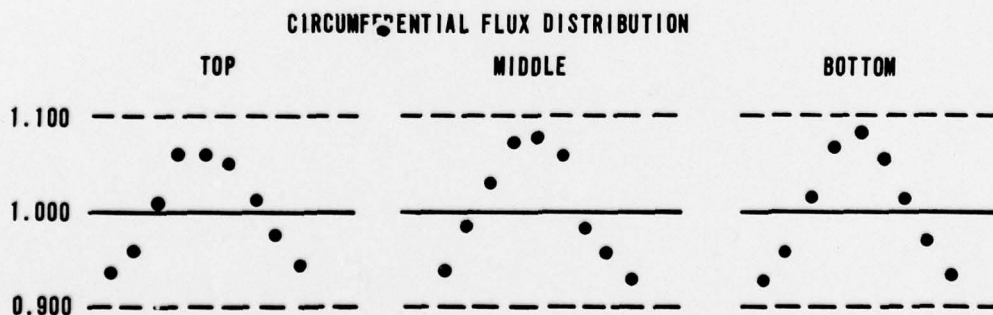
Device	$I_{CBO}$ 10Vcb	$I_{EBO}$ 3Vbc	$I_{CEO}$ 10Vce		$I_{CBO}$ 10Vcb	$I_{EBO}$ 3VEE	$I_{CEO}$ 10Vce
A	na	pa	$\mu a$	B	$\mu a$	na	$\mu a$
2	321 141	125	2.53 1.21	2	23.8 8.46	65.4 110	603 260
4	415 402	19.5 3.19	3.25 1.97	4	12.5 8.49	8.27 9.3	544 178
6	477 240	270	4.60 2.45	6	6.56 3.69	4.02 4.06	192 147
8	122 75	26.4 12.8	3.12 2.12	8	8.00 1.46	2.5 1.1	675 123
10	480 470	35	7.56 8.60	10	3.84 3.27	.556 .306	134 113
12	156 102	222 386	3.26 3.17	12	1.21 .402	2.21 1.53	295 103

## APPENDIX G

## FLUX INFORMATION ON THERMAL COLUMN PNEUMATIC TUBE FACILITY (REF. 17)



Cu(Cd) RATIO=3415 WITH CENTER GRAPHITE BLOCKS OUT  
 ABSOLUTE NEUTRON FLUX  $= 1.6 \times 10^{11} \text{ n} \cdot \text{cm}^{-2} \cdot \text{sec}^{-1}$



17. Becker, D. A., "Flux Information on Thermal Column Pneumatic Tube Facility," an unpublished data sheet available from the National Bureau of Standards, Reactor Operations Division, Gaithersburg, Maryland, June 1971.



## APPENDIX H

## DERIVATION OF THE RELATIVE DAMAGE EQUATION

One measure of relative effectiveness of thermal neutrons to fast neutrons in producing damage in transistors would be the ratio of the thermal neutrons bulk damage constant to the fast-neutron bulk damage constant. Recall the bulk damage equation

$$\Delta(1/\beta) = C\phi$$

Since  $\Delta(1/\beta)$  is a measure of the lattice defects (Recombination Centers) in the base region,  $C$ , the bulk damage constant, must be a measure of the defects produced in the base region per neutron.

Recall that the number of reactions that occur as a result of a fast-neutron irradiation is

$$R = \Sigma \phi V$$

where  $R$  is the reactions,  $\Sigma$  is the macroscopic cross section,  $\phi$  is the neutron fluence, and  $V$  is the volume in which the reactions occur. Recall also that the macroscopic cross section is given by

$$\Sigma = N \sigma$$

where  $N$  is the atom density and  $\sigma$  is the microscopic cross section. Thus, it can be seen that the number of 1 MeV neutron reactions that occur in the base region of a transistor would be

$$R = \sigma_{1 \text{ MeV Si}} N_{\text{Si}} \phi V$$

Define  $u_{1 \text{ MeV}}$  as the defects per fast neutron (1 MeV); then the fast-neutron bulk damage constant would be given by

$$C_{1 \text{ MeV}} = u_{1 \text{ MeV}} \sigma_{1 \text{ MeV Si}} N_{\text{Si}} V_{\text{base}}$$

For the thermal neutron case, the neutron reactions take place in the emitter region, while the gain degrading damage is done by the lithium nucleus and the alpha particle in the base region. The geometry factor ( $G$ ) derived in appendix B gives the particles doing damage in the base region per reaction in the emitter region. Thus, the thermal neutron bulk damage constant would be given by

$$C_{\text{thermal}} = (U_{\alpha} G_{\alpha} + U_{\text{Li}} G_{\text{Li}}) \sigma_{\text{thermB10}} N_{\text{B10}} V_{\text{Emitter}}$$

As long as the combined width of the emitter region and the base region is less than the path length of the lithium recoil,  $G_{\alpha}$  and  $G_{\text{Li}}$  should remain in the same ratio. For this case it should be possible to factor out from the quantity in parenthesis an average number of defects per particle (alpha or lithium). Calling this average  $U_{\text{thermal}}$ , it follows that

$$C_{\text{thermal}} = U_{\text{thermal}} (G_{\alpha} + G_{\text{Li}}) \sigma_{\text{thermB10}} N_{\text{B10}} V_{\text{Emitter}}$$

and

$$\frac{C_{\text{thermal}}}{C_{1\text{MeV}}} = \frac{U_{\text{thermal}} (G_{\alpha} + G_{\text{Li}}) \sigma_{\text{thermB10}} N_{\text{B10}} V_{\text{Emitter}}}{U_{1\text{MeV}} \sigma_{1\text{MeV}} N_{\text{Si}} V_{\text{base}}}$$

$\frac{U_{\text{thermal}}}{U_{1\text{MeV}}}$  was experimentally found to be approximately 1/3.3 or 0.30 as is

indicated in section IV. Also, since the areas of the base and the emitter are equal, the areas would divide out of the relative damage equation. The result is

$$\frac{C_{\text{thermal}}}{C_{1\text{MeV}}} = \frac{0.3 (G_{\alpha} + G_{\text{Li}}) \sigma_{\text{thermB10}} N_{\text{B10}} W_{\text{Emitter}}}{\sigma_{1\text{MeV}} N_{\text{Si}} W_{\text{base}}}$$

where  $W$  is the width of the region.

## DISTRIBUTION LIST

### DEPARTMENT OF DEFENSE

Defense Communication Engineer Center  
ATTN: Code R410, James W. McLean  
ATTN: Code R320, C. W. Bergman

Director  
Defense Communications Agency  
ATTN: Code 930, Monte I. Burgett, Jr.  
ATTN: Code 540.5  
ATTN: Code 430

Defense Documentation Center  
Cameron Station  
12 cy ATTN: TC

Commander  
Defense Electronic Supply Center  
ATTN: ECS, Joe W. Dennis

Director  
Defense Intelligence Agency  
ATTN: DB-4C, Edward O'Farrell  
ATTN: DS-4A2

Director  
Defense Nuclear Agency  
ATTN: DDST  
ATTN: RAEV  
ATTN: STVL  
2 cy ATTN: STVL, LTC W. Adams  
3 cy ATTN: TITL, Tech. Library

Dir. of Defense Rsch. & Engineering  
ATTN: S&SS (OS)

Commander, Field Command  
Defense Nuclear Agency  
ATTN: FCPR

Director  
Interservice Nuclear Weapons School  
ATTN: Document Control

Director  
Joint Strat. Tgt. Planning Staff, JCS  
ATTN: JLTW-2

Chief  
Livermore Division, Field Command, DNA  
Lawrence Livermore Laboratory  
ATTN: FCPRL

Director  
National Security Agency  
ATTN: Orlando O. Van Gunten, R-425

OJCS/J-3  
ATTN: J-3, RDTA Br., WWMCCS, Plans Div.

### DEPARTMENT OF THE ARMY

Project Manager  
Army Tactical Data Systems  
U.S. Army Electronics Command  
ATTN: Dwaine B. Huewe  
ATTN: DRCPN-TDS-SD

### DEPARTMENT OF THE ARMY (Continued)

Commander  
BMD System Command  
ATTN: BDMSC-TEN, Noah J. Hurst

Chief C-E Services Division  
U.S. Army Communications Cmd.  
ATTN: CEE0-7, Wesley T. Heath, Jr.

Commander  
Frankford Arsenal  
ATTN: SARFA-FCD, Marvin Elnick

Commander  
Harry Diamond Laboratories  
ATTN: DRXDO-RBH, Paul A. Caldwell  
ATTN: DRXDO-EM, Robert E. McCoskey  
ATTN: DRXDO-TI, Tech. Lib.  
ATTN: DRXDO-RC, Robert B. Oswald, Jr.  
ATTN: J. Halpin  
ATTN: DRXDO-EM, R. Bostak  
ATTN: J. McGarrity  
ATTN: DRXDO-RB, Joseph R. Miletta  
ATTN: DRXDO-NP, Francis N. Wimenitz  
ATTN: DRXDO-EM, J. W. Beilfuss  
ATTN: DRXDO-TR, Edward E. Conrad  
ATTN: DRXDO-RCC, John A. Rosado

Commanding Officer  
Night Vision Laboratory  
ATTN: CPT Allan S. Parker

Commander  
Picatinny Arsenal  
ATTN: SARPA-ND-N  
ATTN: SARPA-TS-I-E, Abraham Grinock  
ATTN: SMUPA-ND-D-B, Edward J. Arber  
ATTN: SMUPA-ND-N-E  
ATTN: SMUPA-ND-W

Commander  
Redstone Scientific Information Ctr.  
U.S. Army Missile Command  
3 cy ATTN: Chief, Documents

Secretary of the Army  
ATTN: ODUSA or Daniel Willard

Director  
TRASANA  
ATTN: ATAA-EAC, Francis N. Wenaas

Director  
U.S. Army Ballistic Research Labs.  
ATTN: DRXBR-X, Julius J. Meszaros  
ATTN: DRXBR-VL, John W. Kinch  
ATTN: DRXBR-VL, Robert L. Harrison

Commander  
U.S. Army Communications Cmd.  
ATTN: ACC-FD-M, Lawrence E. Cork

Chief  
U.S. Army Communications Sys. Agency  
ATTN: SCCM-AD-SV, Library



DEPARTMENT OF THE ARMY (Continued)

Commander

U.S. Army Electronics Command

ATTN: DRSEL-PL-ENV, Hans A. Bomke  
ATTN: DRSEL-CE, T. Preiffer  
ATTN: DRSEL-TL-IR, Edwin T. Hunter  
ATTN: DRSEL-CT-HDK, Abraham E. Cohen  
ATTN: DRSEL-GG-TD, W. R. Werk  
ATTN: DRSEL-NL-D

Commandant

U.S. Army Engineer School

ATTN: ATSE-CTD-CS, C. S. Grazier

Commander in Chief

U.S. Army Europe and Seventh Army

ATTN: ODCSE-E, AEAGE-PI

Commandant

U.S. Army Field Artillery School

ATTN: ATSFA-CTD-ME, Harley Moberg

Commander

U.S. Army Materiel Dev. & Readiness Cmd.

ATTN: DRCDE-D, Lawrence Flynn

Commander

U.S. Army Missile Command

ATTN: DRCPM-PE-EA, Wallace O. Wagner  
ATTN: DRCPM-LCEX, Howard H. Henriksen  
ATTN: DRSMI-RGD, Vic Ruwe

Commander

U.S. Army Mobility Equip. R&D Ctr.

ATTN: AMSEL-NV-SD, J. H. Carter  
ATTN: STSFB-MW, John W. Bond, Jr.

Chief

U.S. Army Nuc. and Chemical Surety Gp.

ATTN: MOSG-ND, Maj Sidney W. Winslow

Commander

U.S. Army Nuclear Agency

ATTN: ATCN-W, LTC Leonard A. Sluga

Commander

U.S. Army Security Agency

ATTN: IARD-T, Robert H. Burkhardt

Commander

U.S. Army Tank Automotive Command

ATTN: DRCPM-GCM-SW, Lyle A. Wolcott  
ATTN: DRSTA-RHM, 1LT Peter A. Hasek

Commander

U.S. Army Test & Evaluation Comd.

ATTN: DRSTE-NB, Russel R. Galasso  
ATTN: DRSTE-EL, Richard I. Kolchin

Commander

U.S. Army Training & Doctrine Comd.

ATTN: ATORI-OP-SD

Commander

White Sands Missile Range

ATTN: STEWS-TE-NT, Marvin P. Squires

DEPARTMENT OF THE NAVY

Chief of Naval Research

ATTN: Code 427

DEPARTMENT OF THE NAVY (Continued)

Commanding Officer

Naval Avionics Facility

ATTN: Branch 942, D. J. Repass

Commander

Naval Electronic Systems Command

Naval Electronic Systems Cmd, Hqs.

ATTN: Code 504511, Charles R. Suman

ATTN: Code 50451

ATTN: PME 117-21

ATTN: Elex. 05323, Cleveland F. Watkins

ATTN: Code 5032, Charles W. Neill

Director

Naval Research Laboratory

ATTN: Code 2627, Doris R. Folen

ATTN: Code 4104, Emanuel L. Brancato

ATTN: Code 7701, Jack D. Brown

ATTN: Code 5216, Harold L. Hughes

ATTN: Code 6601, E. Wolicki

ATTN: Code 6631, James C. Ritter

ATTN: Code 5210, John E. Davey

ATTN: Code 6440, George Sigel

Commander

Naval Sea Systems Command

ATTN: SEA-9931, Riley B. Lane

ATTN: SEA-9931, Samuel A. Barham

Commander

Naval Ship Engineering Center

ATTN: Code 617402, Edward F. Duffy

Officer-in-Charge

Naval Surface Weapons Center

ATTN: Code 431, Edwin B. Dean

ATTN: Code WA52, R. A. Smith

ATTN: Code WA501, Navy Nuc. Prgms. Off.

ATTN: Code WA50

Commander

Naval Weapons Center

ATTN: Code 533, Tech. Lib.

Commanding Officer

Naval Weapons Evaluation Facility

ATTN: Code ATG, Mr. Stanley

Commanding Officer

Naval Weapons Support Center

ATTN: Code 70242, Joseph A. Munarin

ATTN: Code 7024, James Ramsey

Director

Strategic Systems Project Office

ATTN: SP-2701, John W. Pitsenberger

ATTN: NSP-27331, Phil Spector

ATTN: NSP-230, David Gold

ATTN: NSP-2342, Richard L. Coleman

DEPARTMENT OF THE AIR FORCE

AF Aero-Propulsion Laboratory, AFSC

ATTN: POE-2, Joseph F. Wise

AF Institute of Technology, AU

ATTN: ENP, Charles J. Bridgman

DEPARTMENT OF THE AIR FORCE (Continued)

AF Weapons Laboratory, AFSC

ATTN: ELC  
ATTN: ELA  
ATTN: ELXT  
ATTN: ELS  
ATTN: NTS  
ATTN: DEX  
ATTN: HO, Dr. Minge  
2 cy ATTN: SUL  
5 cy ATTN: ELP, Maj Chronister

AFTAC

ATTN: TFS, Maj Marion F. Schneider

Air Force Avionics Laboratory, AFSC

ATTN: DHE, H. J. Hennecke  
ATTN: DHM, C. Friend  
ATTN: DH, Lt Col McKenzie  
ATTN: AAT, Mason Friar

AUL (LDE)

ATTN: LDE

Commander

ASD

ATTN: ASD-YH-EX, Lt Col Robert Leverette  
ATTN: ENACC, Robert L. Fish

Headquarters

Electronic Systems Division/DC

ATTN: DCKE, Lewis Staples

Headquarters

Electronic Systems Division/YS

ATTN: YSEV

Headquarters

Electronic Systems Division/YW

ATTN: YWEI

Commander

Foreign Technology Division, AFSC

ATTN: ETD/PDJC  
ATTN: ETD

Commander

Rome Air Development Center, AFSC

ATTN: RBRAC, I. L. Krulac  
ATTN: RBRP, Clyde Lane

Commander

Rome Air Development Center, AFSC

ATTN: ETS, R Dolan  
ATTN: ETS, A. Kahan  
ATTN: ET, R. Buchanan

SAMSO/DY

ATTN: DYS, Maj Larry A. Darda

SAMSO/IN

ATTN: IND, I. J. Judy

SAMSO/MN

ATTN: MNNH  
ATTN: MNNG  
ATTN: MNNG, Capt David J. Strobel

DEPARTMENT OF THE AIR FORCE (Continued)

SAMSO/RS

ATTN: RSMG  
ATTN: RSSE

SAMSO/SK

ATTN: SKF

SAMSO/SZ

ATTN: SZJ

Commander in Chief

Strategic Air Command

ATTN: XPFS, Capt Deraad  
ATTN: NRI-Stinfo Library

DEPARTMENT OF ENERGY

University of California

Lawrence Livermore Laboratory

ATTN: Joseph E. Keller, Jr., L-125  
ATTN: Hans Kruger, L-96 (Class L-94)  
ATTN: Tech. Info. Dept. L-3  
ATTN: Lawrence Cleland, L-156  
ATTN: Donald J. Meeker, L-545 (Class L-153)

Los Alamos Scientific Laboratory

ATTN: Doc. Con. for J. Arthur Freed  
ATTN: Doc. Con. for Bruce W. Noel

Sandia Laboratories

ATTN: Doc. Con. for Org. 1933, F. N. Coppage  
ATTN: Doc. Con. for Org. 2110, J. A. Hood  
ATTN: Doc. Con. for Org. 2140, R. Gregory  
ATTN: Doc. Con. for 3141, Sandia Rpt. Coll.

Department of Energy

Albuquerque Operations Office

ATTN: Document Control for WSSB

OTHER GOVERNMENT AGENCY

Department of Commerce

National Bureau of Standards

ATTN: Judson C. French

DEPARTMENT OF DEFENSE CONTRACTORS

Aerojet Electro-Systems Co.

Div. of Aerojet-General Corporation

ATTN: Thomas D. Hanscome

Aerospace Corporation

ATTN: J. Benveniste  
ATTN: Irving M. Garfunkel  
ATTN: John Ditre  
ATTN: Julian Reinheimer  
ATTN: Library  
ATTN: S. P. Bower

Analog Technology Corporation

ATTN: John Joseph Baum

Avco Research & Systems Group

ATTN: Research Lib. A830, Rm. 7201

The BDM Corporation

ATTN: T. H. Neighbors

DEPARTMENT OF DEFENSE CONTRACTORS (Continued)

The BDM Corporation  
ATTN: D. R. Alexander

The Bendix Corporation  
Communication Division  
ATTN: Document Control

The Bendix Corporation  
Research Laboratories Division  
ATTN: Max Frank  
ATTN: Mgr. Prgm. Dev., Donald J. Niehaus

The Bendix Corporation  
Navigation and Control Group  
ATTN: George Gartner

The Boeing Company  
ATTN: Howard W. Wicklein, MS 17-11  
ATTN: Itsu Amura, 2R-00  
ATTN: Aerospace Library  
ATTN: Robert S. Caldwell, 2R-00  
ATTN: Carl Rosenberger, 2R-00

Booz-Allen and Hamilton, Inc.  
ATTN: Raymond J. Chrisner

Brown Engineering Company, Inc.  
ATTN: John M. McSwain, MS 18

Burroughs Corporation  
Federal and Special Systems Group  
ATTN: S. E. Gluck

California Institute of Technology  
Jet Propulsion Laboratory  
ATTN: J. Bryden  
ATTN: A. G. Stanley

Charles Stark Draper Laboratory, Inc.  
ATTN: Paul R. Kelly  
ATTN: Kenneth Fertig

Cincinnati Electronics Corporation  
ATTN: C. R. Stump

Computer Sciences Corporation  
ATTN: Richard H. Dickhaut

Control Data Corporation  
ATTN: Jack Meehan

Cutler-Hammer, Inc.  
AIL Division  
ATTN: Central Tech. Files, Anne Anthony

University of Denver  
Colorado Seminary  
Denver Research Institute  
ATTN: Sec. Officer for Fred P. Venditti

Dikewood Industries, Inc.  
ATTN: L. Wayne Davis

E-Systems, Inc.  
Greenville Division  
ATTN: Library 8-50100

Effects Technology, Inc.  
ATTN: Edward John Steele

DEPARTMENT OF DEFENSE CONTRACTORS (Continued)

Fairchild Camera and Instrument Corp.  
ATTN: Sec. Dept. for 2-233, David K. Myers

Fairchild Industries, Inc.  
Sherman Fairchild Technology Center  
ATTN: Mgr. Config. Data & Standards

Ford Aerospace & Communications Corp.  
ATTN: Samuel R. Crawford, MS 531  
ATTN: Edward R. Hahn, MX-X22  
ATTN: Donald R. McMorrow, MS G30

Ford Aerospace & Communications Operations  
ATTN: Tech. Info. Section  
ATTN: Ken C. Attinger  
ATTN: E. R. Poncelet, Jr.

The Franklin Institute  
ATTN: Ramie H. Thompson

Garrett Corporation  
ATTN: Robert E. Weir, Dept. 93-9

General Dynamics Corp.  
Electronics Div., Orlando Operations  
ATTN: D. W. Coleman

General Electric Company  
Space Division  
ATTN: John L. Andrews  
ATTN: Joseph C. Peden, VFSC, Rm. 4230M  
ATTN: Larry I. Chasen

General Electric Company  
Re-Entry & Environmental Systems Div.  
ATTN: Robert V. Benedict  
ATTN: John W. Palchefskey, Jr.

General Electric Company  
Ordnance Systems  
ATTN: Joseph J. Reidl

General Electric Company  
TEMPO-Center for Advanced Studies  
ATTN: DASIAC  
ATTN: M. Espig  
ATTN: Royden R. Rutherford

General Electric Company  
Aircraft Engine Business Group  
ATTN: John A. Ellerhorst, E 2

General Electric Company  
Aerospace Electronics Systems  
ATTN: Charles M. Hewison, Drop 624  
ATTN: W. J. Patterson, Drop 233

General Electric Company  
ATTN: David W. Pepin, Drop 160

General Electric Company-TEMPO  
ATTN: DASIAC for William Alfonte

General Research Corporation  
ATTN: Robert D. Hill

Georgia Institute of Technology  
Georgia Tech. Research Institute  
ATTN: R. Curry



DEPARTMENT OF DEFENSE CONTRACTORS (Continued)

Georgia Institute of Technology  
Office of Contract Administration  
ATTN: Res. & Sec. Coord. for Hugh Denny

Grumman Aerospace Corporation  
ATTN: Jerry Rogers, Dept. 533

GTE Sylvania, Inc.  
Electronics Systems Grp-Eastern Div.  
ATTN: Charles A. Thornhill, Librarian  
ATTN: James A. Waldon  
ATTN: Leonard L. Blaisdell

GTE Sylvania, Inc.  
ATTN: H&V Group  
ATTN: Paul B. Fredrickson  
ATTN: Charles H. Ramsbottom  
ATTN: Herbert A. Ullman

Gulton Industries, Inc.  
Engineered Magnetics Division  
ATTN: Engr. Magnetics Div.

Harris Corporation  
Harris Semiconductor Division  
ATTN: Wayne E. Abare, MS 16-111  
ATTN: T. L. Clark, MS 4040  
ATTN: Carl F. Davis, MS 17-220

Hazeltine Corporation  
ATTN: Tech. Info. Ctr., M. Waite

Honeywell Incorporated  
Avionics Division  
ATTN: Ronald R. Johnson, A1622  
ATTN: R. J. Kell, MS S2572

Honeywell Incorporated  
Avionics Division  
ATTN: MS 725-J, Stacey H. Graff  
ATTN: MS 725-5A, Harrison H. Noble

Honeywell Incorporated  
Radiation Center  
ATTN: Technical Library

Hughes Aircraft Company  
ATTN: Kenneth R. Walker, MS D157  
ATTN: John B. Singletary, MS 6-D133  
ATTN: Billy W. Campbell, MS 6-E-110

Hughes Aircraft Company, El Segundo Site  
ATTN: William W. Scott, MS A1080  
ATTN: Edward C. Smith, MS A620

IBM Corporation  
ATTN: Frank Frankovsky

IIT Research Institute  
ATTN: Irving N. Mindel

Int. Tel. & Telegraph Corporation  
ATTN: Alexander T. Richardson

ION Physics Corporation  
ATTN: Robert D. Evans

DEPARTMENT OF DEFENSE CONTRACTORS (Continued)

IRT Corporation  
ATTN: R. L. Mertz  
ATTN: MDC  
ATTN: Ralph H. Stahl  
ATTN: Leo D. Cotter

Jaycor  
ATTN: Catherine Turesko  
ATTN: Robert Sullivan

Johns Hopkins University  
Applied Physics Laboratory  
ATTN: Peter E. Partridge

Kaman Sciences Corporation  
ATTN: W. Foster Rich  
ATTN: Walter E. Ware  
ATTN: Jerry I. Lubell  
ATTN: Donald H. Bryce  
ATTN: Albert P. Bridges

Litton Systems, Inc.  
Guidance & Control Systems Division  
ATTN: Val J. Ashby, MS 67  
ATTN: John P. Retzler

Lockheed Missiles & Space Co., Inc.  
ATTN: George F. Heath, D/81-14  
ATTN: Edwin A. Smith, Dept. 85-85  
ATTN: Benjamin T. Kimura, Dept. 81-14  
ATTN: L. Rossi, Dept. 81-64  
ATTN: Samuel I. Taimuty, Dept. 85-85

Lockheed Missiles & Space Co., Inc.  
ATTN: Tech. Info. Ctr. D/Coll.

MIT Lincoln Laboratory  
ATTN: Leona Loughlin, Librarian, A-082

Martin Marietta Aerospace  
Orlando Division  
ATTN: William W. Mras, MP-413  
ATTN: Jack M. Ashford, MP-537  
ATTN: Mona C. Griffith, Lib. MP-30

Martin Marietta Corporation  
Denver Division  
ATTN: Paul G. Kase, Mail 8203  
ATTN: Research Lib. 6617, Jay R. McKee  
ATTN: J. E. Goodwin, Mail 0452

McDonnell Douglas Corporation  
ATTN: Tom Ender  
ATTN: Technical Library

McDonnell Douglas Corporation  
ATTN: Stanley Schneider

McDonnell Douglas Corporation  
ATTN: Technical Library, C1-290/36-84

Mission Research Corporation  
ATTN: William C. Hart

Mission Research Corporation  
ATTN: David E. Merewether

Mission Research Corporation-San Diego  
ATTN: J. P. Raymond  
ATTN: V. A. J. Van Lint

DEPARTMENT OF DEFENSE CONTRACTORS (Continued)

The Mitre Corporation  
ATTN: M. E. Fitzgerald

National Academy of Sciences  
ATTN: National Materials Advisory Board for  
R. S. Shane

University of New Mexico  
Electrical Engineering & Computer Science Dept.  
ATTN: Harold Southward

Northrop Corporation  
Electronic Division  
ATTN: Boyce T. Ahlport

Northrop Corporation  
Northrop Research & Technology Ctr.  
ATTN: J. R. Srouer  
ATTN: Orlie L. Curtis, Jr.  
ATTN: David N. Pocock

Northrop Corporation  
Electronic Division  
ATTN: John M. Reynolds  
ATTN: Vincent R. DeMartino  
ATTN: Joseph D. Russo

Palisades Inst. for Rsch. Services, Inc.  
ATTN: Records Supervisor

Physics International Company  
ATTN: Doc. Con. for Charles H. Stallings  
ATTN: Doc. Con. for John H. Huntington

R&D Associates  
ATTN: S. Clay Rogers  
ATTN: William R. Graham, Jr.

Raytheon Company  
ATTN: Gajanan H. Joshi, Radar Sys. Lab.

Raytheon Company  
ATTN: Harold L. Mescher

RCA Corporation  
Government Systems Division  
Astro Electronics  
ATTN: George J. Brucker

RCA Corporation  
David Sarnoff Research Center  
ATTN: K. H. Zaininger

RCA Corporation  
Camden Complex  
ATTN: E. Van Keuren, 13-5-2

Research Triangle Institute  
ATTN: Eng. Div., Mayrant Simons, Jr.

Rockwell International Corporation  
ATTN: Donald J. Stevens, FA70  
ATTN: K. F. Hull  
ATTN: James E. Bell, HA10  
ATTN: N. J. Rudie, FA53  
ATTN: George C. Messenger, FB61  
ATTN: L. Apodaca, FA53

DEPARTMENT OF DEFENSE CONTRACTORS (Continued)

Rockwell International Corporation  
ATTN: T. B. Yates

Rockwell International Corporation  
Collins Division  
ATTN: Dennis Sutherland  
ATTN: Mildred A. Blair  
ATTN: Alan A. Langenfeld

Sanders Associates, Inc.  
ATTN: Moe L. Aitel, NCA 1-3236

Science Applications, Inc.  
ATTN: Larry Scott  
ATTN: J. Robert Beyster

Science Applications, Inc.  
ATTN: J. Roger Hill

Simulation Physics, Inc.  
ATTN: Roger G. Little

The Singer Company (Data Systems)  
ATTN: Tech. Info. Center

Sperry Flight Systems Division  
Sperry Rand Corporation  
ATTN: D. Andrew Schow

Sperry Rand Corporation  
Sperry Division  
ATTN: Charles L. Craig, EV  
ATTN: Paul Maraffino

Sperry Univac  
ATTN: James A. Inda, MS 41T25

Stanford Research Institute  
ATTN: Philip J. Dolan

Stanford Research Institute  
ATTN: MacPherson Morgan

Sundstrand Corporation  
ATTN: Curtis B. White

Systron-Donner Corporation  
ATTN: Gordon B. Dean  
ATTN: Harold D. Morris

Texas Instruments, Inc.  
ATTN: Donald J. Manus, MS 72

TRW Defense & Space Sys. Group  
ATTN: Robert M. Webb, R1-2410  
ATTN: H. H. Holloway, R1-2036  
ATTN: Tech. Info. Center/S-1930  
2 cy ATTN: O. E. Adams, R1-1144  
2 cy ATTN: R. K. Plebuch, R1-2078

TRW Defense & Space Sys. Group  
San Bernardino Operations  
ATTN: R. Kitter  
ATTN: F. B. Fay

TRW Systems Group  
ATTN: Donald W. Pugsley

DEPARTMENT OF DEFENSE CONTRACTORS (Continued)

United Technologies Corporation  
Hamilton Standard Division  
ATTN: Raymond G. Giguere

Vought Corporation  
ATTN: Technical Data Ctr.

DEPARTMENT OF DEFENSE CONTRACTORS (Continued)

Vought Corporation  
Michigan Division  
ATTN: Tech. Lib.

Westinghouse Electric Corporation  
Defense & Electronics Systems Ctr.  
ATTN: Henry P. Kalapaca, MS 3525